DESIGN AND SIMULATION OF KALMAN FILTER FOR ESTIMATION OF GAS TURBINE INLET TEMPERATURE

BY

USEN, FRANCIS FRANCIS
20194175558

A THESIS SUBMITTED TO THE
DEPARTMENT OF ELECTRICAL AND ELECTRONIC ENGINEERING,
FEDERAL UNIVERSITY OF TECHNOLOGY,
OWERRI, IMO STATE, NIGERIA

IN PARTIAL FULFILLMENT OF THE REQUIREMENTS FOR THE AWARD OF MASTER OF ENGINEERING (M.ENG) IN CONTROL ENGINEERING.

AUGUST, 2024

CERTIFICATION

CERTIFICATION

This is to certify that this thesis on Design and Simulation of Kalman Filter for Estimation of Gas Turbine Inlet Temperature was carried out by **Usen, Francis Francis** with registration number: 20194175558.

Engr. Dr. S. E. Mbonu
(Supervisor)
30/07/2025
Date

Engr. Dr. S. O. Okozi
(Co-Supervisor)
30/07/2025
Date

Engr. Prof. N. Chukwuchekwa
(Head, Department of Electrical and Electronic Engineering)
21/9/25
Date

Engr. Prof. M. C. Ndinechi
(Dean, School of Electrical Systems & Engineering Technology)
Date

Prof. (Mrs.) J. N. Nwosu
(Dean, Post Graduate School)
Date

Engr. Prof. E. Omorogiuwa
(External Examiner)
Date

DEDICATION

I dedicate this research work to the Holy One of Israel, for His mighty Hand in my education.

ACKNOWLEDGEMENTS

First and foremost, I would like to thank the Almighty God for His grace, wisdom, and academic endowment. I am deeply grateful for the strength He provided throughout my journey, enabling me to successfully complete this program while supporting my family along the way.

I extend my profound gratitude to my esteemed Supervisors, Engr. Dr. S. E. Mbonu and Engr. Dr. S. O. Okozi, for their invaluable encouragement, insightful advice, scholarly support, and meticulous review of this project. Your mentorship has been instrumental in the completion of this work. I also wish to honor my late former Supervisor, Associate Professor C. C. Mbaocha, whose vision, tutelage, and academic guidance laid a strong foundation for the success of this project.

I sincerely appreciate the corporate sacrifices of the Head of Department, Engr. Prof. N. Chukwuchekwa, and the Deans, Engr. Prof. M. C. Ndinechi and Prof. (Mrs.) J. N. Nwosu. Your dedication to our academic progress, including your unwavering commitment to moderating project defenses, has been priceless.

I am equally grateful to the following lecturers whose teachings and support have contributed significantly to my academic development: Engr. Profs. D. O. Dike, J. O. Onojo, Engr. Drs. L. O. Uzoechi, I. O. Akwukwaegbu, M. Olubiwe, O. C. Nosiri, J. K. Obichere, L. S. Ezema and S. O. Okozi. I sincerely appreciate each one of you.

A heartfelt thank you goes to my family, whose unwavering support has been a cornerstone of my academic and personal life. To my wonderful wife, Princess Rosemary, you have been my perfect match, providing love and strength in every aspect of my life. I am equally grateful to my energetic sons, Abraham and Isaac, for their patience and understanding throughout the writing of this report. To my brothers, Mr. Ezekiel and Mr. Anthony Usen, their wives, Mrs. Unyime Ezekiel and Mrs. Edidiong Anthony, and my sisters, ObongAnwan Stella Usen, Mrs. Edima Ndaobong, Mrs. Franca Mbaba, Pst. Felicia Usen, and Mrs. Rita Usoro, your constant encouragement and support have been invaluable. I also acknowledge my in-laws, Mr. Benjamin Ndaobong, Mr. Koko Mbaba, Mr. Idorenyin Usoro, and my nephews and nieces for their continued love and care. Also, to my late parents, late Patron F. A. U. Usen and late Mrs. Rita F. Usen, may God reward you in eternity.

I really appreciate my colleagues at NetcoDietsmann company limited, and my contemporaries at the Federal University of Technology, Owerri. Thank you, and God bless you all.

LIST OF FIGURES

LIST OF TABLES

LIST OF PLATES

NOMENCLATURE

ABBREVIATIONS

ABB	Asean Brown Boveri
ANFIS	Adaptive Neuro-Fuzzy Inference System
ANN	Artificial Neural Network
AMPC	Adaptive Model Predictive Control
APC	Advanced Process Control
ASC	Adaptive Synergetic Controller
DSE	Dynamic State Estimation
EKF	Extended Kalman Filter
ESFOA	Enhanced Sunflower Optimization Algorithm
GT	Gas Turbine
HDGT	Heavy-Duty Gas Turbine
I	Identity Matrix
IC	Internal Combustion
IPP	Independent Power Plant
KF	Kalman Filter
Li-Ion	Lion Lithium
LTI	Linear Time Invariant
MIMO	Multiple Input Multiple Output
MIPS	Medium-Voltage Integrated Power System.
MNV	Measurement Noise Variance
MPC	Model Predictive Control
MPP	Maximum Point Power
MSSA	Modified Salp Swarm Algorithm
MW	Megawatts
NAOC	Nigerian Agip Oil Company

NASA	National Aeronautics & Space Administration
NCP	Numerical Current Prediction
NDAE	Nonlinear Differential Algorithm Equation
NMPC	Nonlinear Model Predictive Control
NO	Nitrate Monoxide
NO_2	Nitrogen Dioxide
NOx	Nitrate Oxides
ODE	Ordinary Differential Equation
OEM	Original Equipment Manufacturer
PF	Particle Filter
PID	Proportional-Integral-Derivative
PMU	Phasor Measurement Unit
PNV	Process Noise Variance
PV	Photo-Voltaic
RAUKF	Robust Adaptive Unscented Kalman Filter
RMSE	Root Mean Square Error
RNN	Recurrent Neural Networks
SCADA	Supervisory Control And Data Acquisition
SE	State Estimation
SSA	Salp Swarm Algorithm
SSE	Static State Estimation
SoC	State of Charge
TAT	Temperature After Turbine
TIT	Turbine Inlet Temperature
TSE	Tracking State Estimation
UKF	Unscented Kalman Filter
VIGV	Variable Inlet Guide Vanes

num	Numerator
den	Denominator

VARIABLES

cp	Specific Heat Coefficient (J/kg*K)
f	Fuel-to-Air Ratio
Hv	Lower Heating Value (J/kg)
ma	Air Mass Flow Rate (kg/s)
mf	Fuel Mass Flow Rate (kg/s)
p	Pressure (bar)
P_E	Electrical Output Power (MW)
P	Pressure, Error Covariance
Q	Process Noise Covariance
q	Heat
R	Measurement Noise Covariance
s	Entropy
std	Standard Deviation
T	Temperature (°C)
v	Volume

SYMBOLS

ηt	Thermal Efficiency
Υ	Adiabatic Coefficient
δ	Sigma (Standard Deviation)
E_{th}	Thermal Energy
μ	Mean

TABLE OF CONTENTS

ABSTRACT

The measurement of Gas Turbine (GT) Inlet Temperature remains a significant challenge for engineers, particularly in developing countries, due to the specialized technology required for accurate estimation and covariance noise signal attenuation in remote temperature measurement systems. This technology is primarily utilized by Gas Turbine manufacturers, who employ proprietary, closed-source mathematical models that are inaccessible to external engineers. To address this limitation, the present study develops an open-source model capable of both estimating GT Inlet Temperature and mitigating noise characteristics in the measurement data. The approach is based on the integration of a Kalman Filter (KF) model and a Plant model within a State-Space framework, utilizing real-time input parameters from two identical Gas Turbines, GT11 and GT12, designed by Asea Brown Boveri (ABB). The primary objective is to ensure that the proposed open-source model delivers optimal performance and solution accuracy comparable to that of the closed-source proprietary models. Initially, the Burner Can Temperature Rise Equation is employed to compute the GT Inlet Temperatures directly for the two turbine models. This equation is subsequently used to derive the system matrices in the State-Space representation, which describe the plant model. To complete the modelling, fictitious noise signals are introduced into the plant model and superimposed onto the Kalman Filter model to simulate real-world measurement conditions. The resulting design is implemented and tested in the MATLAB Simulink environment. Simulation results demonstrate that the proposed open-source model achieves accuracies of 98.1% and 97.2% for GT11 and GT12 respectively, when compared to real-time process data from ABB, while the calculated values yield 80% and 65% accuracies, respectively. Furthermore, the fictitious covariance noise signals were successfully filtered from the temperature measurements, confirming the robustness of the proposed model in mitigating noise and enhancing temperature estimation accuracy.

Key words – Kalman Filter, Gas Turbine, Inlet Temperature, State Space, Power Plant, model.

CHAPTER ONE

INTRODUCTION

1.1 Background of Study

Gas Turbines (GT) have been widely used for power generation and other industrial applications in developing countries like Nigeria, because of massive hydrocarbon deposits. Apart from hydrocarbon deposits, the use of Gas Turbines in power generation will continually be prevalent, largely due to high overall efficiencies (Gupta et al., 2007). Gas turbines have proven to be more robust and adaptive to climatic adversities and load variations. Renewable energy sources on the other part may not have the ability to damp disturbances by tripping to safety during critical load variations (Impram et al., 2020). Gas turbines are the type of internal combustion (IC) engines in which the burning of air-fuel mixture produces hot gases to spin a turbine and produce power (Wartsila, 2021). It is mainly designed to extract as much as the energy from the fuel (Asgari, 2014), (Harman, 1981), and (Jonathan et al., 2018). Multiple thermodynamic processes combine to produce the overall complex output power of a gas turbine. In this complexity, various process variables can be measured directly, while many other variables are not available for direct measurement. These remote variables that cannot be directly measured, but can rather be inferred or estimated based on the system outputs measured by sensors (Mathworks, 2024). In order to achieve effective process control, higher performance, efficiency and reliability, unknown states must be determined from sensor data (Venkateswarlu and Karri, 2022). In line with this, some thermodynamic parameters associated with the input materials must be considered during modeling. Atmospheric conditions must also be factored into the measurement. Measurement biases and model uncertainties are part of this design. Indirect measurement of an unknown State of a system through the filter method is termed State Estimation (Duan and Li, 2020). The concept of State Estimation has seriously concentrated around the output power and transmission only. Accurate parameter estimations

play major roles in diagnostics, process control and safety considerations (Venkateswarlu and Karri, 2022). In the process of Estimation, the model used should be capable of mitigating measurement noise covariance and model errors. This is only possible with an Advanced Process Control (APC) technology. Advanced Process Control (APC) is a comprehensive scheme that leverages sophisticated algorithms, mathematical models and advanced control strategies to predict, optimize and improve industrial processes for efficiency, reliability, safety and productivity (ABB, 2024). The APC control scheme is a more sophisticated form of process control scheme that goes beyond the limitations of the legacy PID control schemes (Zero Instrument, 2024). With APC, the Kalman Gain (K) is calculated internally by the system using process dynamics and sensor updates (Franklin, 2020).

As Hou et al. in 2018 put it, the increasing emphasis on the efficiency, safety and cleanliness of the power generation process makes it significantly important to put forward advanced control strategies to satisfy the desired control demand of the gas turbine system. Power generation with gas turbine is a complex, nonlinear process. Meanwhile there are several processes that are either linear or nonlinear within the complex system. Turbine Inlet temperature measurement can be assumed a linear process when considered in isolation.

Different Advanced Process Control (APC) models have been used to estimate unknown states of a dynamic system in literatures. Impraimakis and Smyth, in 2022 used Unscented Kalman Filter (UKF) while Haji et al., in 2020 used Adaptive Model Predictive Control (AMPC) schemes for state estimations at different instances. Other APC models in the literature include Artificial Neural Networks (ANN), Adaptive Synergetic Control (ASC), Particle Filter (PF), Recurrent Neural Networks (RNN) etc. In all these, mathematical computations with arbitrary data still flood the research space. In the industrial space, the Original Equipment Manufacturers (OEM) continually play monopoly of parameter estimations using proprietary models. In order to break this monopoly, an open-source model is used to estimate the Turbine

Inlet Temperature (TIT) using the same real – time process data obtained from two OEM plants. A thorough analysis of the input parameters, measurement and noise distributions, as well as the combined cycle process is done in chapter two of this work in order to give a better understanding of the system's behavior. In the Gas Turbine (GT) internal combustion process, the two major input parameters which are atmospheric air and fuel gas, along with some known constants are used to configure a known Kalman Filter (KF) model. The filter is an open – source model. In this work, the TIT will be estimated by simulating the proposed Kalman Filter (KF) model in a SIMULINK environment. The results will be compared to the temperature estimates obtained from an OEM model. The combustion temperature ranges between 700^0C to 1700^0C, with specific value depending on some process factors (Salim et al., 2020). Temperature extremes result in material damage, fuel wastage and gaseous emissions. Since every measured state has some process and measurement noise covariance signals with it, Kalman filter not only measures, but filters out spurious signals from the measurement spectrum. It presents an optimal temperature estimate.

In the gas turbine system, process transmitters are used to convert the physical quantities measured by sensors into standardized electrical signals (Zero Instrument, 2024). These transmitters are turbine flow transmitters, temperature transmitters and pressure transmitters. The Advanced Process Control model integrates the multiple data sources from the different transmitters to form a more useful and accurate data structure. Intermittent sensor noise can have great impact on the system performance (Rafi et al., 2017). The noise progresses along the signal path to the adaptive element of the controller. The Kalman Filter is a control framework that can handle noise signals while delivering the process.

1.2 Problem Statement

Gas turbine (GT) manufacturers are tasked with defining critical design parameters during the production phase, one of which is the Turbine Inlet Temperature (TIT). Accurate estimation of

TIT is essential, yet it presents significant challenges due to the extreme operating conditions within the combustion chamber. Direct measurement of the TIT is impractical because of the high turbulence and extreme temperatures present in the combustion environment. These conditions introduce substantial measurement uncertainties and noise, making physical sensing unreliable or impossible. As a result, Original Equipment Manufacturers (OEMs), such as Asean Brown Boveri (ABB), General Electric (GE), etc, employ advanced estimation models to predict the TIT while filtering out noise in real time. However, these models are proprietary and not accessible for external use. Although several academic and open-source estimation models exist, they are largely untested in real-time industrial applications. This creates a gap in practical implementation, particularly for engineers in developing countries, where access to closed-source technologies is limited. The lack of transparency and accessibility in TIT estimation techniques hinder broader participation in GT design and manufacturing, thereby restricting innovation and technological advancement in under-resourced regions.

1.3 Objectives of Study

The major objective of this research is to design and simulate Kalman Filter for estimation of Gas Turbine Inlet Temperature. In order to achieve this major objective, the research effort shall be geared towards the following specific objectives.

i. To develop the System Matrices for State Space implementation.
ii. To characterize a Kalman Filter model using the System Matrices.
iii. To simulate the Kalman Filter model and validate the results using MATLAB Simulink.

1.4 Significance of Study

This research aims to explore the potential application of the Kalman Filter in the operation of Gas Turbines. The significance of this work lies in its capacity to challenge the current dominance of temperature measurement and control technologies, which are primarily

controlled by foreign manufacturers. By validating the Kalman Filter for use in Gas Turbine operations, this study offers a promising alternative to conventional methods, thereby promoting greater technological autonomy. The outcomes of this research hold particular relevance for engineers and researchers in developing nations, as well as for independent Gas Turbine manufacturers, who may face challenges due to the reliance on proprietary temperature control systems. If successfully implemented, the Kalman Filter could contribute to enhanced operational efficiency and greater control over Gas Turbine systems, providing substantial cost benefits and reducing dependency on foreign technology.

1.5 Scope of Study

This study focuses on state-space modelling for the estimation of a single unknown state variable within the internal combustion section of a gas turbine system. It does not encompass the estimation of overall output power or other secondary energy conversion processes. The internal combustion process is analysed in isolation, decoupled from the broader and more complex turbine dynamics. The thermodynamic burner can temperature rise equation is employed to derive the system matrices required for the state-space formulation. These matrices, in conjunction with known parameters of the gas turbine, are utilized to implement a Kalman Filter for real-time state estimation. The gas turbine models used in this research are the Alstom (Class F) GT11 and GT12 models—150 MW single-shaft power turbines equipped with annular combustors and operating in open cycle mode. These turbines were originally designed by Asea Brown Boveri (ABB – Power) and are currently operated by the Nigerian Agip Oil Company (NAOC), located in Delta State, Nigeria. Real-time operational data for the study were sourced from an Independent Power Plant situated in Delta State, providing practical validation for the modelling and estimation techniques applied in this research.

CHAPTER TWO

LITERATURE REVIEW

2.1 Overview of Gas Turbine

A Gas Turbine (GT) consists of multiple interconnected process loops that combine to form a complex and sophisticated nonlinear system. Each individual loop relies on the proper functioning of others to ensure smooth and efficient operation. Gas Turbines consist of four primary components namely; air compressor, combustion chamber, turbine and exhaust module (Testbook, 2023). These components work in unison to compress air, mix it with fuel for combustion, and subsequently expand the hot gases to generate power. The efficient operation of these components is supported by an intricate network of instrumentation and control systems (Biswas, 2024).

Since the operation of each process loop is interdependent, any changes in one loop can have significant effects on others, ultimately impacting the overall cycle. A key challenge in GT operation is the measurement of the Turbine Inlet Temperature (TIT), as it involves high temperatures and difficult physical access (Tree et al., 2022).

The process of power generation in a Gas Turbine follows the Brayton Cycle. Plate 2.1 provides a cross-sectional view of a Gas Turbine, illustrating the various stages of the Brayton Cycle, starting with the Air Inlet, where atmospheric air is continuously drawn into the system (Whittle et al., 2025). The air is then compressed in the Compressor stage, which utilizes a system of steel blades arranged radially around a central shaft. Between the Compressor and the Gas Generator Turbine, Inlet Guide Vanes regulate the flow of compressed air into the Combustion Chamber. The next stage involves the Power Turbine or Gas Generator Turbine, which consists of a set of limited radial blades where the energy transformation takes place before the exhaust phase.

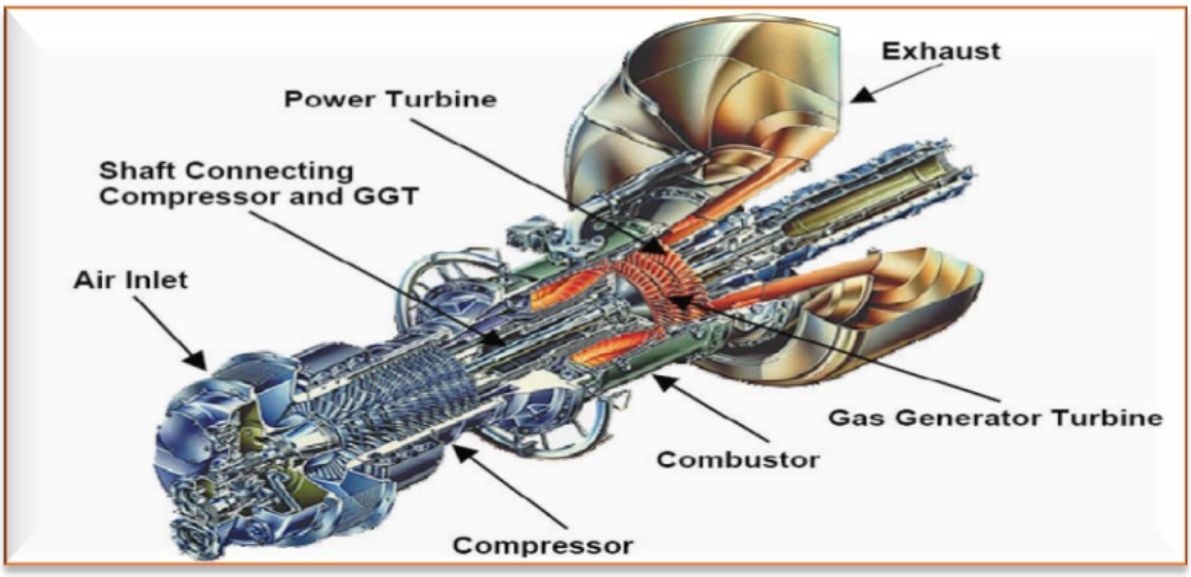

Plate 2.1: A Typical Gas Turbine Engine (Kurz and Ohanian, 2003)

2.1.1 Brayton Cycle

The Brayton Cycle, also called Joule Cycle, is the thermodynamic cycle upon which all gas turbines operate (Brooks, GER-3567H). This cycle was first proposed by George Brayton in 1870 (Högnäs, 2005). The cycle is a continuous combustion cycle with five sections namely; air-intake, compression, combustion, turbine-cycle and exhaust. The Brayton Cycle efficiently uses high temperature gases from a combustion process, but discharges its exhaust gas at a relatively high temperature. As shown in figure 2.1, the Brayton or Joule cycle is commonly used to analyse the gas turbine systems, using thermodynamic properties (Pathirathna, 2013). The end product of the Brayton Cycle is the generation of enormous thermal energy needed to produce thrust or mechanical motion for aircrafts and GT respectively.

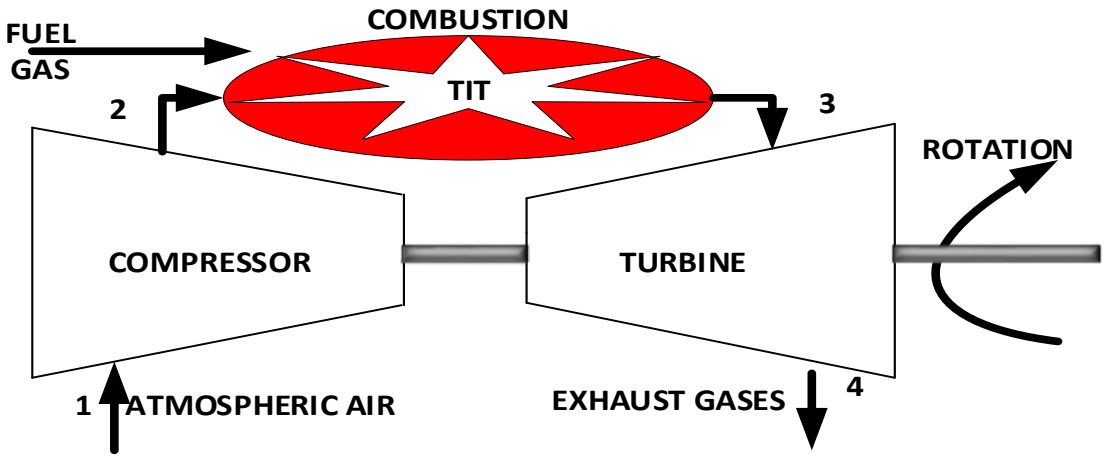

Fig 2.1: The Brayton Cycle (Zohuri, 2018)

Exit guide vanes further diffuse the compressed air before releasing it into the igniters in the combustion chamber, where it is mixed with ignition gas in a flame tube. Two igniters with integral temperature measurement probes are provided. A thermocouple is fitted to each igniter. Ignition gas is usually a propane gas, which has a smaller molecular weight.

An ignition transformer supplies a high voltage power through the igniters to produce sparks which ignite the gas/air mixture in the flame tube. The thermocouples sense satisfactory ignition of the gas/air mixture. Temperature measurement of the internal engine stops at the ignition temperature. The three components of fire triangle are complete in the combustion engine. Once the ignition flame is established, the heavy molecule fuel gas takes over with full combustion. The specific heating value of the gas determines the air/gas ratio (RealPars, 2019). Other factors that determine the air/gas ratio are the quality of air, moisture content, altitude from sea level. The flame travels beyond the flame tube and bursts out through a set of annular combustors and strike the turbine vanes with a swirl. This causes turbulence and produces great torque on the turbine vanes when all the combustors have been put to service. At this level, the ignition gas is cut off, and the turbine inlet temperature or firing temperature is established. The turbine vanes spin to maximum speed as the firing temperature ramps up due to continuous injection of fuel gas and compressed air. Used gases diffuse through the turbine exhaust end at

a temperature which measures up nearly 500^0C. This exhaust end temperature can also be called Temperature After Turbine (TAT). As the engine fires on, high pressure jets of fire continue to strike the turbine blades.

Figures. 2.2 explain each part of the Brayton cycle where; P = pressure, V = volume, q = heat, S = entropy and T = temperature. The Pressure or Compression Ratio of the Brayton Cycle is shown in figure 2.2b. It is defined as the ratio of the stagnation pressure as measured at the front and rear of a gas turbine (Pratt and Whitney, 1982). A high-pressure ratio increases the engine's weight, and causes the air to heat up faster as it passes from one compressor stage to another. It increases the inlet temperature, and compressor efficiency, and adds value to the output power. Compression ratio is useful in determining the turbine inlet temperature, as well as the turbine output power (Ibrahim and Rahman, 2012).

I. **1-2:** isentropic compression in the inlet and compressor

II. **2-3:** isobaric combustion with heat gain

III. **3-4:** isentropic expansion in the turbine blades and exhaust

IV. **4-1:** isobaric air cooling with heat rejection

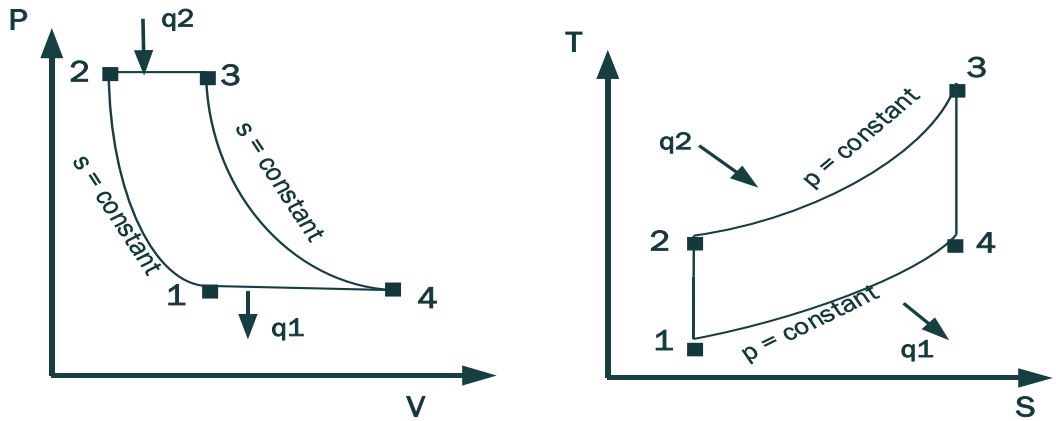

Fig.2.2: (a) P – V diagram (Proctor II, 2003) (b) T – S diagram (Proctor II, 2003)

2.1.2 Fuel Gas

Fuel gas is a key factor in the design and operation of the gas turbine. There is the need to know the details of the fuel gas, based on its characteristics to guarantee the performance of the gas

turbine (RealPars, 2019). Natural gas is widely used as fuel gas in power generation. Its hydrocarbon constituents are as shown on Table 2.1. It is primarily obtained from industrial process and treated in a gas processing plant far away from the power plant. It is then transported to a power plant through the launching trap systems. A gas pig launcher transfers the processed fuel gas from the gas plant to the power plant, while a gas pig receiver receives the transported fuel gas at the power plant area. At the receiving end, the fuel gas is again scrubbed, pre-heated and de-pressurized at a small treatment plant before being distributed into two or three different gas manifolds to form parallel gas streams. This combination forms the fuel gas distribution system. The fuel gas is filtered and applied into the combustion chamber of the gas turbine through two or three control valves. These valves regulate the flow of the fuel gas coming from the different gas streams at a constant pressure. Energy demand determines the quantity of fuel gas throttled into the combustion engine at all times.

Table 2.1 shows the different components of the natural gas used as fuel gas. Methane gas has the highest molecular mass, followed by Ethane, Propane and Carbon-dioxide gases. The percentage of carbon dioxide is always monitored and kept to the minimum during fuel gas processing. Carbon-dioxide is the only component that is observed on a special computer monitor. The more the percentage by mol of carbon dioxide, the more likely the turbine flame would extinguish. In order to maintain a healthy flame, proper gas treatment is carried out at the Gas Processing Plant. Burnes and Camon, 2019 maintain that Natural Gas is superior to other fossil fuels with lower hydrogen-carbon ratios in terms of carbon emissions, power and efficiency.

Table 2.1: Natural Gas Composition for Fuel Gas (NAOC, 2024).

S/N	Gas	Symbol	(%mol) GT11	(%mol) GT12
01	Nitrogen	N_2	0.48778	0.46453
02	Carbon-dioxide	CO_2	2.86204	2.78779
03	Methane	CH_4	81.98425	82.13406
04	Ethane	C_2H_6	7.41690	7.51425
05	Propane	C_3H_8	4.12751	4.09724
06	I-Butane	C_4H_{10}	1.16877	1.13468
07	N-Butane	C_4H_{10}	0.92365	0.89989
08	N-Pentane	C_5H_{12}	0.22400	0.21284
09	I-Pentane	C_5H_{12}	0.35737	0.34526
10	Hexane	C_6H_{14}	0.21252	0.19436
11	Heptane	C_7H_{16}	0.15823	0.14471
12	Octane	C_8H_{18}	0.07698	0.07040

2.1.3 Atmospheric Air.

Every internal combustion engine requires the availability of compressed air to complete the process. The Brayton cycle starts with the introduction of atmospheric air into the compressor duct. Once the generator rotor is excited, the compressor rotates from standstill and begins to suck the atmospheric air. The air is filtered in two stages (NAOC, 2006). Firstly, by inlet coalescer which blocks any fine liquid droplets and corrosive chemicals. Secondly, by a system of programmable pulse air filters arranged in rows and columns to remove most of the particulate matter from the inlet air. The pulse filters then direct clean air into the compressor inlet casting. The volume of air entering the compressor is controlled by Variable Inlet Guide Vanes (VIGV). The VIGV opens to take in air into the compressor duct, and into the combustion chamber. The vanes are operated by a hydraulically-operated linear actuator

(NAOC, 2006). The amount of opening is measured in degrees, by two measurement angle transmitters attached to the VIGV. The VIGV gives circumferential velocity to the air at the inlet before delivering it to the compressor (Boyce, 2006).

The axial air compressor consists of some rows of stator blades that are in line with the same rows of rotor blades (Boyce, 2006). A compressor stage is a set of stator and rotor rows as a combination. Air flow enters the compressor blades axially (parallel to its rotation), and exits in the same axial direction. As the air is accelerated by the rotor blades, and diffused in the stator blades, air compression is achieved (Boyce, 2012). The compressor blades reduce in size from the first region to the third and exit region of the axial compressor.

2.1.4 Gas Turbine Cooling

The Gas Turbine is a constant-volume machine, where a constant mass flow of air will pass through the inlet duct (SPE, 2023). If the ambient temperature increases, the density of the inlet air decreases, and the air mass flow rate reduces, thereby reducing the overall GT efficiency, which comes as an increase in compressor power consumption. This is followed by a corresponding decrease in the output power. The GT inlet air cooling can be achieved by direct evaporative system or indirect evaporative system (Yousef and Abubakar, 2015). Direct cooling or indirect cooling is to improve GT performance. According to researchers, extra output power is achieved during compressor cooling.

2.1.5 Review of GT Parameters

Various process parameters for this study were derived from the process plants, while certain other parameters were from theoretical formulations. These formulations were obtained as special parameters associated with the standard process variables used for Gas Turbine power generation such as air and fuel gas. Their individual contribution to the Temperature estimation has been handled in details.

2.1.5.1 Turbine Inlet Temperature (TIT)

Turbine Inlet Temperature or Firing Temperature is the highest temperature attained in the system (Basu and Debnath, 2019). From figure 2.2, the highest temperature of the cycle is at point *T3*. This is the temperature at the first-stage nozzles of the gas turbine. The TIT increases with the fuel gas flow rate. According to (Aminov et al., 2018), increase in GT Inlet Temperature produces a corresponding increase in the thermal and thermodynamic efficiencies of the Brayton Cycle. However, higher TIT significantly increases the thermal stress in the metals, which affects the life of the components (Aminov et al., 2018) and (Gupta et al., 2007). At such temperatures, gaseous emissions certainly occur. On the other hand, lower TIT may cause low efficiencies and low load conditions (Gupta et al., 2007). To this end, the TIT values are fixed by Turbine Manufacturers. The is TIT not available for measurement, and so requires specialized technologies and other sundry advanced control strategies for its estimation. The combustion chamber is a hostile environment. Typically, it is achieved by control systems approximation. The turbine exhaust temperature, which is an accessible parameter can also be used to confirm the value of the inlet temperature to avoid over-firing.

2.1.5.2 Thermal Efficiency (η_t)

Thermal efficiency of the Brayton Cycle represents the fraction of heat converted to work, after a portion of the heat has been dissipated as waste. It is the ratio of the work it does to the input heat at the high temperature (Nuclear-Power, 2025). Thermal efficiency of the Brayton Cycle can be expressed in terms of temperatures or pressure ratio. This research work expresses the Thermal efficiency in terms of compressor pressure ratio. There are other engine efficiencies, but this research work focuses on thermal efficiency of the Brayton Cycle because Turbines and compressors operate under adiabatic conditions, meanwhile they are idealized as isentropic for calculation purposes. An adiabatic process, without friction, is called an isentropic process (Menon, 2011).

2.1.5.3 Adiabatic Index (Υ)

Adiabatic index is also known as Heat Capacity Ratio is the ratio of heat capacity at constant pressure to the heat capacity at constant volume (*cp*/*cv*) (Aakash, 2021). It can as well be called isentropic expansion factor and is denoted by Υ (gamma) for ideal gas or κ (kappa) for a real gas (Hellacioussatyr, 2024). Heat Capacity at constant pressure is always higher than Heat Capacity at constant volume (Subramaniam, 2018). At constant pressure, the amount of heat added does some work and therefore increases the internal energy of the system, thereby changing the volume. Meanwhile at constant volume, the amount of heat added to the system increases the pressure with increased temperature without doing any work. The internal energy of the system keeps increasing. More heat is added at constant pressure than at constant volume. The resultant heat capacity ratio is greater than one. In (Mukherjee, 2021) short explanation, the adiabatic index is a special case in which no heat exchange occurs between the system and its surroundings. According to the author, it indicates how much work an adiabatic system can extract with its internal energy without any external supply. For diatomic gases, $\Upsilon = 1.4$.

2.1.5.4 Specific Heat Coefficient of Air (*cp*)

The specific heat of a gas is a measure of the amount of energy necessary to raise the temperature of the gas by a single degree (NASA, 2023). The amount depends on the process used to raise the temperature. There is a specific heat coefficient at constant volume (cv), and a specific heat coefficient at constant Pressure (cp). The ratio of the two coefficients (cp/cv) is the Adiabatic Index (gamma) as earlier discussed. The specific heat coefficient is related to its internal energy, which is the sum of the kinetic and potential energies of its constituent particles. When a substance is heated, the energy is absorbed by the particles, which increases their kinetic energy and raises the temperature of the substance. The specific heat coefficient determines how much energy is required to achieve a given temperature change. The specific heat coefficient of air is 1.005KJ/(kg*K).

2.1.5.5 Compressor Pressure Ratio $(P2/P1)$

This is of the most important parameters that relates to gas turbine performance and efficiency. The axial gas turbine compressor takes in excess air from the atmosphere into the air inlet compartment. The compressed air is for two purposes. Much compressed air is used for cooling and dilution of the combustion gases. A little portion of the compressed air is mixed with the fuel gas and used for the actual combustion (CSA, 2013). The gas turbine pressure ratio is the ratio of the total pressure at the exit of the compressor stage to the total pressure at the inlet of the compressor stage in a gas turbine engine. A high-pressure ratio indicates that the compressor is able to compress the air more effectively, resulting in higher temperatures and pressures in the combustion chamber. This leads to more efficient combustion and a greater expansion of the hot gases in the turbine, which in turn produces more power.

2.1.5.6 Fuel-to-Air Ratio: $f = (mf/ma)$

The amount of fuel flowing into the combustion chamber of the gas turbine is measured by a turbine flow meter as mass flow *(mf)* in kg/sec. Mass is never created nor destroyed, and it's neither affected by temperature or pressure changes during the process. Flow measurement in terms of mass flow is preferred for accuracy (Sundén and Fu, 2017). In the same way, the amount of air drawn into the compressor duct *(ma)* is calibrated in kg/sec by the manufacturer's nozzle design as earlier explained. The ratio of the fuel mass flow rate to the calibrated air mass flow rate into the combustors is the fuel-to-air ratio. It typically ranges from 1:10 to 1:40. This means that for every 40kg of air, 1kg of fuel is consumed. Fuel-to-air ratios are designed by Original Equipment Manufacturers (OEM). This is obtained in the orifices in the head-end of the combustor, and the fuel gas orifices in the fuel nozzle. The ratio depends on the fuel type, operating conditions and turbine design (CSA, 2013). Heavy gas turbines are designed to operate with a ratio of 1:15 theoretically. The actual values for the parameters used for this

research work are obtained in design calculations of chapter three, estimated at 1:32 and 1:36 for GT11 and GT12 respectively.

From figure 2.3, as the pressure ratio $(P2/P1)$ increases, the thermal efficiency (η_t) increases and the output power (P_E) also increases. The output power experiences a diminishing return at a critical pressure ratio. The solution is to trade some output power in order to improve the efficiency. Since the inlet temperature is fixed, increasing the output power is achieved by performing some manipulations around the pressure ratio, mass flow rate of the fuel gas and the efficiency.

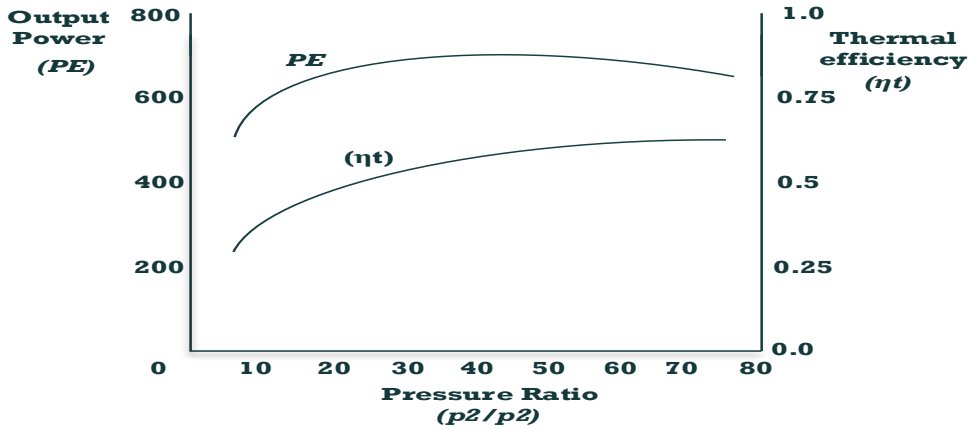

Fig 2.3: Power and Thermal Efficiency Curves (Weber, 2019).

2.1.5.7 Lower Heating Value of Fuel Gas (Hv)

This is the amount of heat released when the fuel gas is completely burned, and the products of combustion are cooled to the initial temperature of the gas and the surroundings. It accounts for the energy contained in the chemical bonds of the fuel gas. The water vapor from the combustion remains in its gaseous state. The lower heating value changes with process dynamics. It is a function of the fuel used. According to (Battista et. al., 1982), Fuel-to-Air ratio increases with decreasing heating value of fuel in order to mix large quantities of fuel with the air to provide acceptable combustion.

2.2 Overview of Kalman Filter (KF)

The Kalman filter, developed by Rudolf E. Kalman, is an algorithm used to estimate the state of a given system using other measurement data. It is used to compute hidden states from observation (Ahmed, 2023). It estimates the State of a system from noisy measurements (Pearson, 2016). In its operation, it combines noisy sensor outputs to estimate the system state with uncertain dynamics. Kalman filters are very fast, making them great tools for embedded systems and real time problems. According to (Biezen, 2015), it is an iterative mathematical process that uses a set of equations and consecutive data inputs to quickly estimate the true value of the object being measured, under unpredicted or random error. In (Ahmed, 2023) explanation, the Kalman filter is an Optimal Estimator for linear systems, and a recursive data processing algorithm that works in a predictor-corrector fashion. It does not accumulate history excepting its immediate previous state. Kalman Filter is a model-based control scheme implemented in State Space. The model captures the relationships between process variables, system's dynamics, and constraints (Instool, 2023) for prediction, optimization and decision-making. The variables of interest can only be measured indirectly or by observation. The Kalman filter can handle a multiple-input / multiple-output (MIMO) system (Ulusoy, 2018). With its robust algorithm and multiple sensor information it can predict the unknown temperature of a process, while filtering noisy signals from the sensors and the process. Kalman filter combines the measurement and its prediction to find an optimal estimate of the state. The estimate minimizes any quadratic loss function of estimation (Ahmed, 2023).

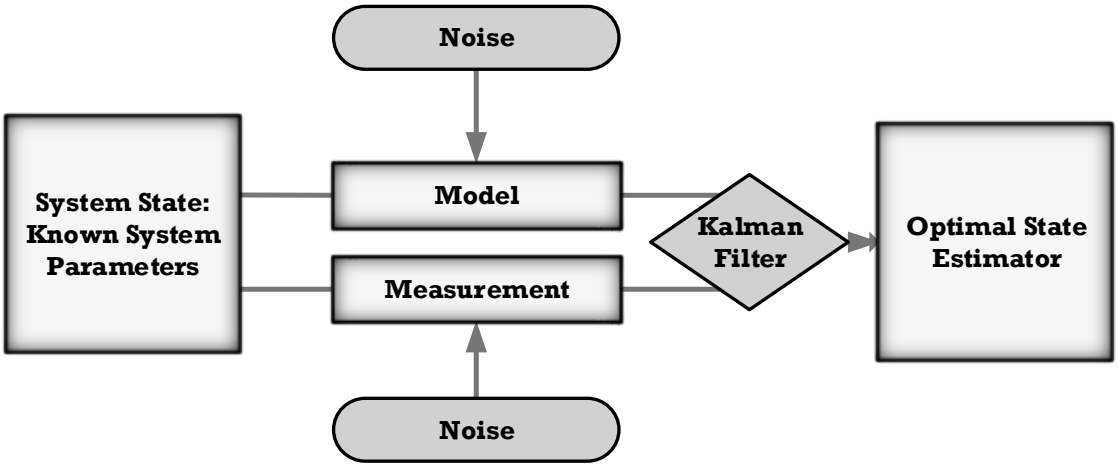

Fig. 2.4: Block diagram of Kalman Filter (Ahmed, 2023).

2.2.1 Kalman Filter Operation.

The Kalman filter operates in two stages. The system model is first used to calculate the a-priori state estimate ($\hat{x}_k^-$) and the error covariance, P (Ulusoy, 2018). P is a measure of uncertainty in the estimated state. This is the prediction stage. The second stage of the algorithm uses the a-priori estimate obtained in the prediction stage to update them to find a-posteriori estimate ($\hat{x}_k$) of the system state and the error covariance. For standard Kalman filtering, everything must be linear. Assuming the following information from the Gas Turbine:

Gas Turbine Dynamics: $x_k = Ax_{k-1} + Bu_k + w_k$ (2.1)

Sensor Measurements: $y_k = Cx_k + v_k$ (2.2)

The mathematical model has the following:

Model Equation: $\hat{x} = A\hat{x}_{k-1} + Bu_k$ (2.3)

Model Uncertainties: $\hat{y} = C\hat{x}_k$ (2.4)

Where;

w_k = process noise with covariance Q,

v_k = measurement noise with covariance R.

χ_k = state vector of the real plant

y_k = plant output

u_k = plant input vector

$\hat{x}_k$ = estimated model state

$\hat{y}_k$ = estimated model output.

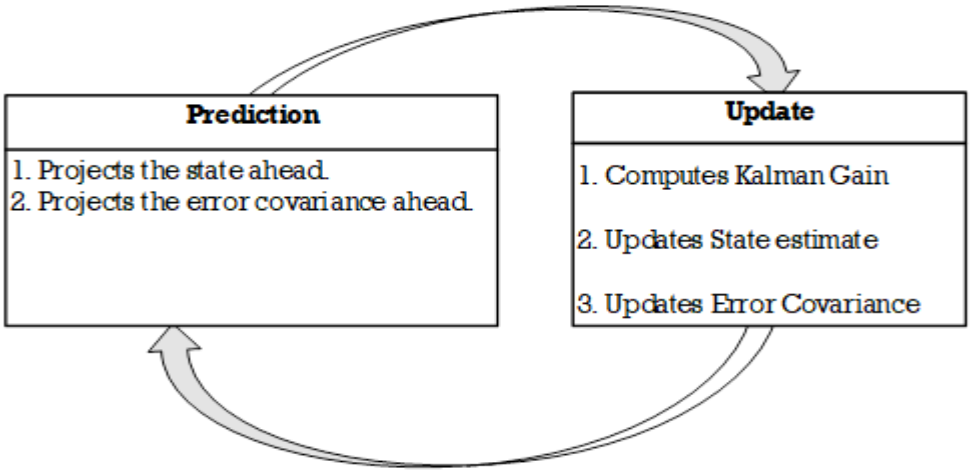

Fig. 2.5: Prediction – Update Diagram (Ahmed, 2023).

The optimal estimate is found by multiplying the prediction and measurement probability functions together, scaling the result and computing the mean of the resulting probability density function (Ulusoy, 2018).

The Kalman Filter Equation is embedded in the Filter. The Kalman Filter combines the system state and the system state error covariance with measurement parameters to establish its model equations as follows:

1. Initialization:

   i. system state estimate = x_0

   ii. system state error covariance = P_0

2. Re-initialization:

   i. System state estimate = x_{k-1}

   ii. System state error covariance = P_{k-1}

3. Prediction (a-priori):

   i. $$\hat{x}^-_k = A\hat{x}_{k-1} + Bu_k + w_k \quad (2.5)$$

   ii. $$P_k^- = A\,P_{k-1}\,A^T + Q_k \quad (2.6)$$

4. Kalman Gain:

$$K_k = P_k^- C^T \left(C\,P_k^- C^T + R\right)^{-1} \quad (2.7)$$

$$K_k = P_k^- C^T / (C P_k^- C^T + R) \quad (2.8)$$

5. Updates from Measurements and previous estimates (a-posteriori):

i. $$\hat{x}_k = \hat{x}_k^- + K_k (y_k - C\hat{x}_k^-) \quad (2.9)$$

ii. $$P_k = P_k^- - K_k C P_k^- \quad (2.10)$$

$$P_k = (1 - K_k C) P_k^- . \quad (2.11)$$

The above Kalman Model equations translate into the following Flowchart.

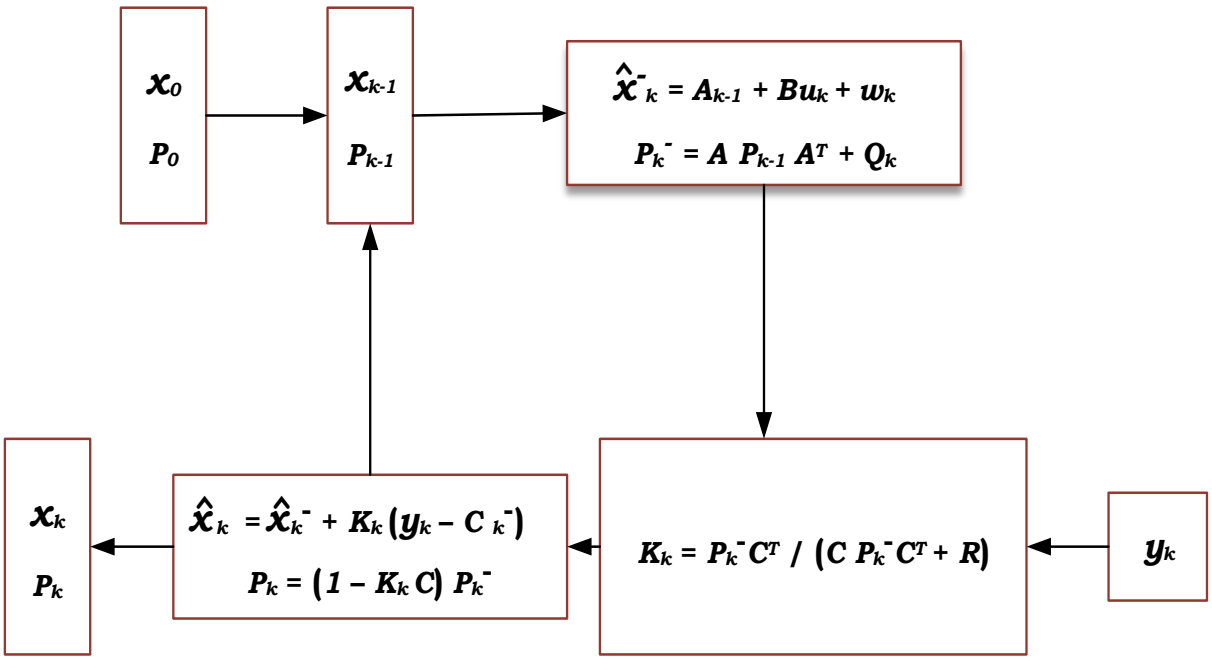

Fig.2.6: Kalman Filter Flowchart Diagram (Biezen, 2015).

2.2.2 Kalman Filter as State Observer.

A State Observer models a real system in order to provide an estimate of the internal state of the system (Vinodh et al., 2013). It is a controller that controls the estimate of a system towards the real system, based on sensor output data (RH, 2018). Any state that is not accessible for direct measurement is estimated by a State Observer. The mathematical model is only an approximation of the real system. The actual system is subject to uncertainties. For any perfect model devoid of uncertainties, and with the real system having the same initial conditions as

the mathematical model, the measurements and the estimated output values must match each other. That is $\hat{y} = y$. Therefore, the estimated initial temperature must match the true initial temperature, such that $\hat{x} = \chi$. Since this is not possible in real life, a State Estimator is used to eliminate the error. It Controller chooses its gain (**K**) in order to minimize the error (***e***) optimally.

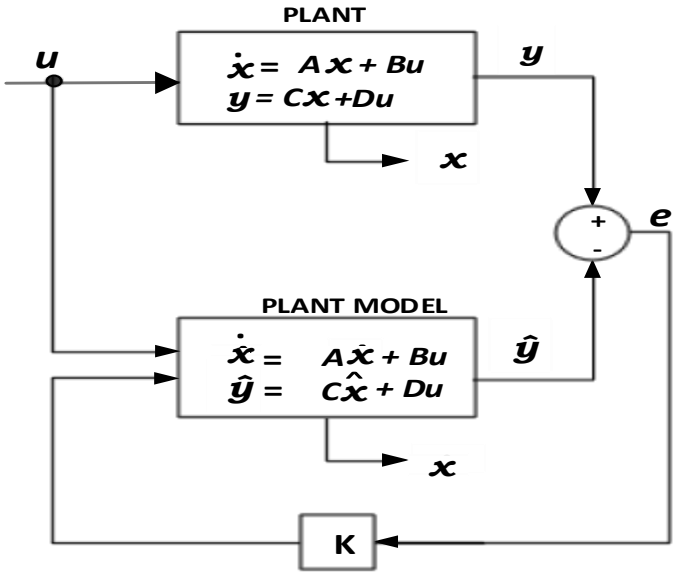

Fig. 2.7: The State Observer (Ulusoy, 2018).

Where:

u = plant input(s)

y = plant output

χ = state of the real plant

A, B, C, D = system matrices from the plant model,

$\hat{y}$ = estimated model output,

$\hat{x}$ = estimated state of the model,

e = error signal,

K = Observer Gain**.**

2.2.3 Derivatives of Kalman Filter.

The Kalman Filter has several derivatives. The following variants of the Kalman Filter have been developed due to different process dynamics. They are mostly for nonlinear processes with more advanced computational capabilities. Other filters developed by other scientists also exist. Such filters have not been mentioned in this work.

2.2.3.1 Extended Kalman Filter (EKF)

The Extended Kalman filter is a non-linear Estimator designed for Gaussian distributions. It is sensitive to minute changes in initial condition of the measurement. It tends to linearize the non-linear function around the mean of the current state estimates (Tiwari, 2015). This linearization results in the computation of Jacobian Matrices used for the prediction. It therefore does not work with discontinuous systems, but with differentiable systems. Meanwhile, its computational cost is low if the Jacobians are computed analytically, but high if computed numerically.

2.2.3.2 Unscented Kalman Filter (UKF)

The UKF is another nonlinear State Estimator that is also designed for Gaussian distributions. UKF has stability issues when approximating square root of covariance matrix. Its computational cost is medium.

2.2.3.3 Particle Filter (PF)

This is similar to the UKF, but with likely arbitrary sampling points. It requires larger number of particles, which can be difficult to handle. Particle filter is the most popular approach (Sudesh et al., 2017). This is because of its flexibility and adaptability. It is a nonlinear process model designed for non-Gaussian distributions. It has a high computational cost.

2.3 Parameter Measurement.

A process of determining how large or small a physical quantity is, as compared to a basic reference quantity of the same kind is called measurement (Young and Freedman, 2012).

Measurements associate numbers with physical quantities and phenomenon. In the course of measurement, independent, randomly generated variables are obtained.

Values will follow a normal distribution with an equal number of measurements above and below the mean value (Dasgupta and Amer, 2013). This distribution is also known as Gaussian Distribution. The Gaussian or Normal distribution is a probability distribution that is symmetrical about the mean, showing that data near the mean are more frequent in occurrence than data far away from the mean (Antai and Chen, 2023). If a distribution is Gaussian, the Mean, Median and Mode are the same and vice versa.

1. The Empirical Rule

Every normal distribution is described by the mean and the standard deviation (Dasgupta and Wahed, 2014). Data falling outside 3δ signify a rare occurrence.

a. Mean ±1δ contains 68.2% of all values.

b. Mean ±2δ contains 95.5% of all values.

c. Mean ±3δ contains 99.7% of all values.

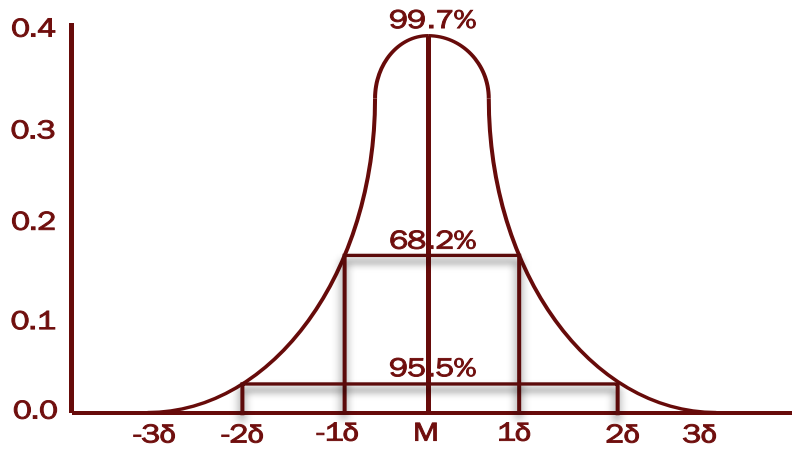

Fig. 2.8: The Gaussian distribution (Dasgupta and Wahed, 2014)

The equation of the normal distribution is given by the normal probability density function (pdf) as follows:

$$P(x) = \frac{1}{\delta\sqrt{2\pi}} e^{-1/2\left(\frac{x-\mu}{\delta}\right)^2} \quad (2.12)$$

Where;

x = variable being examined

P(x) = probability function

μ = mean

δ = sigma (standard deviation)

e = 2.71828

2. Gaussian Noise

Gaussian noise, named after Carl Frederick Gauss, is a term from signal processing theory denoting a kind of signal noise that has a probability density function (pdf) equal to that of a normal or Gaussian distribution (Augustyn, 2023).

Considering the Gaussian Density Function,

$$P(\omega) = \frac{1}{\sqrt{2\pi}} \int_{-\infty}^{\infty} P(x) e^{i\omega x} \; dx \quad (2.13)$$

$$= \frac{1}{\sqrt{2\pi}} \int_{-\infty}^{\infty} \frac{e^{-x^2/2\delta\text{^}2}}{\sqrt{2\pi}\delta} e^{i\omega x} \; dx \quad (2.14)$$

$$= \frac{\delta}{\sqrt{2\pi}} e^{(-1/2)(\omega\delta)\text{^}2} \quad (2.15)$$

For n-dimensional Gaussian distribution $\mathcal{N}(x,$ P), where x is an n-vector and the covariance, P is a (nxn) symmetric positive-definite matrix, the Density function becomes:

$$P(x) = \frac{1}{\sqrt{(2\pi)\text{^}n} * \det \text{ P}} e^{\left(-\frac{1}{2}\right)(x-x)^{\text{T}} * \text{P}\text{^}-1(x-x)} \quad (2.16)$$

$$= \frac{1}{\sqrt{(2\pi)\text{^}n} * \det \text{ P}\text{^}-1} e^{\left(-\frac{1}{2}\right)\omega\text{^T}\omega(x)} \quad (2.17)$$

where, ω is an n-vector.

A noise signal spreads across the real measurement spectrum because it has a probability density function (pdf) similar to the real measurement signal. The noise values are distributed in a normal Gaussian way, just like the normal distribution.

2.4 State Estimation (SE).

Sudev et al., 2017 maintains that State Estimation is a way of approximating the system states by processing the input data. It is the assigning of a value to an unknown system state using the measurement data and system configuration data, based on a criterion. The criterion is to minimize the sum of the squares of the difference between the actual value and the estimated value (Manojkumar et al., 2017). According to (Moura, 2018), State Estimation is the process of determining the internal state of an energy system, by "fusing" a mathematical model and inputs/outputs data measurements. So many remote parameters exist in the industry. Rotor angles, rotor speed, transient voltage, energy expended, enthalpy, state of charge of battery, TIT, etc. Direct measurements with sensors are not always possible. Meanwhile, these parameters are useful in system control.

2.4.1 Static State Estimation (SSE)

The Static State Estimator has an algorithm for calculating the state vector using real-time measurement data obtained from Phasor Measurement Unit (PMU) or a Supervisory Control and Data Acquisition System (SCADA). It uses instantaneous data to estimate the unknown variable for that instant.

2.4.2 Tracking State Estimation (TSE)

The TSE is useful when a control system tends to fluctuate it its output parameters. It comes in during load variations in the power system. It updates the system with output variations, and estimates the state vectors at higher output and lower output conditions.

2.4.3 Dynamic State Estimation (DSE)

The DSE is useful when predicting the state vector for all instances of the control system. It requires the application of PMU technology to constantly generate data from sample of input waveforms.

2.5 State Space Representation

State Space representation is a mathematical model of a physical system showing the relationship between a set of inputs, outputs and state variables by first-order differential equations.

The state of a system describes enough about the system to determine its future behaviour in the absence of any external forces. Position, angular displacement, temperature, orientation, etc., are examples of the states of a system. A collection of these quantities can represent the status of the system. State variables are the smallest set of variables whose values at a time, together with input signals are sufficient to describe the state of the system at any time (Roberts, 2010). They are all the set of values or conditions of the system. Such values include position, speed, temperature, current, voltage, displacement and so forth. The State Vector is a quantity that contains the state variables as its element.

In order to apply Kalman Filter, a system model must be in the State Space form. The Stata Space is a way of representing dynamic systems in time domain. A dynamic system has a set of inputs, u(t), and outputs, y(t). The State variables represent an internal description of the system which completely characterizes the system state at any time, t, and from which any output variables y(t) may be computed. The main aim is to have an equation that shows that the output is a function of the inputs and the states. The mathematical description of any dynamic system is expressed as a set of n-coupled first – order ordinary differential equation (ODE) known as state equations. The time derivative of each state variable is expressed in terms of the state variables and the system inputs and time.

$$\dot{x}_1 = f_1(x, u, t) \tag{2.18}$$

$$\dot{x}_2 = f_2(x, u, t) \tag{2.19}$$

. .

. .

$$\dot{x}_n = f_n(x, u, t) \tag{2.20}$$

(a) Input Equation

Assuming that the system is linear and time – invariant (LTI), then the time derivative of each state variable is expressed in terms of the state variables and the system input:

$$x_1(t) \ldots\ldots\ldots\ldots x_n(t) \tag{2.21}$$

$$u_1(t) \ldots\ldots\ldots\ldots u_r(t) \tag{2.22}$$

$$\dot{x}_1 = a_{11}x_1 + a_{12}x_2 \ldots\ldots\ldots + a_{1n}x_n + b_{11}u_1 + \ldots\ldots\ldots + b_{1r}u_r \tag{2.23}$$

$$\dot{x}_2 = a_{21}x_1 + a_{22}x_2 \ldots\ldots\ldots + a_{2n}x_n + b_{21}u_1 + \ldots\ldots\ldots + b_{2r}u_r \tag{2.24}$$

. .

. .

$$\dot{x}_n = a_{n1}x_1 + a_{n2}x_2 \ldots\ldots\ldots + a_{m}x_n + b_{n1}u_1 + \ldots\ldots\ldots + b_{nr}u_r \tag{2.25}$$

In matrix form,

$$\frac{d}{dt}\begin{bmatrix}\dot{x}_1\\ \dot{x}_2\\ .\\ \dot{x}_n\end{bmatrix} = \begin{matrix}a_{11} & a_{12} \ldots a_{1n}\\ a_{21} & a_{22} \ldots a_{2n}\\ . & . \quad .\\ a_{n1} & a_{n2} \ldots a_{nm}\end{matrix}\begin{matrix}x_1\\ x_2\\ .\\ x_n\end{matrix} + \begin{matrix}b_{11}\ldots\ldots b_{1r} & u_1\\ b_{21}\ldots\ldots b_{2r} & .\\ \ldots\ldots\ldots & .\\ b_{n1}\ldots\ldots b_{nr} & u_r\end{matrix} \tag{2.26}$$

(2.27)

(2.28)

where;

n = no. of states

r = no. of inputs

m = no. of outputs

x = state vector

u = input vector

A = state transition matrix

B = input matrix

The state equation becomes;

$$\dot{x} = Ax + Bu \tag{2.29}$$

The rate of change of a state ($\dot{x}$) is a function of the state (Ax) and input (Bu).

(b) Output Equation

A system's output is defined as any variable of interest. Output may be represented by a linear combination of the state variables (x_i) and the system's input (u_i). An output variable is a system of n-order with r-inputs as follows:

$$y(t) = C_1x_1 + C_2x_2 + \ldots\ldots\ldots\ldots + C_nx_n + D_1u_1 + \ldots\ldots\ldots + D_ru_r \tag{2.30}$$

$$y_1 = C_{11}x_1 + C_{12}x_2 + \ldots\ldots\ldots\ldots + C_{1n}x_n + D_{11}u_1 + \ldots\ldots + D_{1r}u_r \tag{2.31}$$

$$y_2 = C_{21}x_1 + C_{22}x_2 + \ldots\ldots\ldots\ldots + C_{2n}x_n + D_{21}u_1 + \ldots\ldots\ldots + D_{2r}u_r \tag{2.32}$$

. .

$$y_n = C_{m1}x_1 + C_{m2}x_2 + \ldots\ldots\ldots + C_{mn}x_n + D_{m1}u_1 + \ldots\ldots + D_{mr}u_r \tag{2.33}$$

In matrix form,

$$\begin{bmatrix} y_1 \\ y_2 \\ . \\ y_n \end{bmatrix} = \begin{bmatrix} C_{11} & C_{12}\ldots C_{1n} \\ C_{21} & C_{22}\ldots C_{2n} \\ . & \\ C_{m1} & C_{m2}\ldots C_{mn} \end{bmatrix} \begin{bmatrix} x_1 \\ x_2 \\ \\ x_n \end{bmatrix} + \begin{bmatrix} D_{11}\ldots\ldots\ldots D_{1r} & u_1 \\ D_{21}\ldots\ldots\ldots D_{2r} & . \\ . & \\ D_{m1}\ldots\ldots\ldots D_{mr} & u_r \end{bmatrix} \begin{bmatrix} (2.34) \\ (2.35) \\ . \\ (2.36) \end{bmatrix}$$

where;

y = column vector of the output variables

C = matrix of the constant coefficient that weighs the state variables. It is the measurement sensitivity matrix,

D = matrix of the constant coefficient that weighs the system inputs. D reduces to a null matrix mostly, and the output equation reduces to a simple weighted combination of the state variables.

The output equation becomes,

$$y = Cx + Du \tag{2.37}$$

Thus, the output from the model is a function of whatever happens within the system i.e. a function of the state (Cx) and a function of the input (Du). The state space representation of the dynamic system now becomes;

$$\dot{x} = Ax + Bu$$

$$y = Cx + Du$$

2.6 Review of Related Works

Lo et al., 2023 combined two different models to estimate the intrinsic parameters of a Photo Voltaic (PV) panel by means of Current and Voltage (I-V) dynamic monitoring. They observed the output voltage and current after load disturbance. Then an Artificial Neural Network (ANN) model was first used to estimate the PV panel parameters, before later fine-tuning the data with a Numerical Current Prediction (NCP) model to increase accuracy. Their development environment was a solar panel modelled as a set of series and parallel electrical equivalent circuits. The simulation result showed that 6% accuracy of the estimated parameters was achieved. The estimated parameters could now be used for diagnostics and tracking of Maximum Power Point (MPP) of PV panels. This research work relied on arbitrary academic parameters. The practical implementation and stability of this model cannot be ascertained.

Sharifig and Salarieh, 2023 presented a survey for a better control of the exhaust gas temperature and the output power of a Gas Turbine (GT). They understudied the nonlinearity of the entire turbine system to ascertain its controllability. After the survey, an Extended Kalman Filter (EKF) was used to first estimate the GT exhaust gas temperature and shaft speed through their sensors. The estimated parameters were later compensated with the proposed Adaptive Synergetic Controller (ASC). The simulation results, when compared with a parallel

simulation from a classical nonlinear Proportional-Integral (P-I) Controller, proved the superiority of the compensated parameters. The synergetic approach was more effective for parameter estimation and GT controls. This study was rather complex. It combines both linear and nonlinear loops in a single survey which could lead to inaccuracies when handling multiple models.

Nadeem et al., 2022 carried out a comprehensive work on power systems network. They proposed a simple Dynamic State Estimation (DSE) algorithm to jointly estimate the algebraic and dynamic states of a power system using Lyapunov theory. The DSE algorithm utilizes machine dynamics, algebraic constraints and synchronized measurements from Phasor Measurement Units (PMUs) to perform DSE for a complete Nonlinear Differential Algebraic Equation (NDAE) to represent a power system amidst uncertainties. The algebraic variables were the voltage and phase angle of the synchronous generator, while the dynamic states were the rotor angle and the network frequency. Active and reactive power components of the generator formed the algebraic constraints in the model. Ordinary Differential Equations (ODE) described the generator dynamic states, as algebraic equations described the power flow or network constraints and states. These equations combined to get the NDAE representation of the power system network. The well-known Lyapunov theory was finally used to estimate the unknown parameters while designing a robust observer to minimize disturbances, nonlinearities and unknown inputs. Simulation results have shown that the NDAE Observer produced better estimates of the dynamic and algebraic states with good computational efficiency, for different network and machine constraints. This was another complex survey where multiple models were involved. It was also done using arbitrary academic parameters.

Hou et al., 2022 presented a robust model to accurately capture the dynamic states of a synchronous generator in the presence of two major uncertainties. The uncertainties were the measurement noise covariance from the sensors, and the model errors. Their objective was to

filter out the spurious noise signals, compensate for unknown model parameters and then carry out a DSE of the power system states to ascertain safety and reliability of the power system. In the first approach, a robust regression method, called M- Estimator was used to update the measurement noise covariance signal. Then after, the effects of model parameter errors were suppressed using adaptive update method, while considering computational complexity and state estimation requirements. The proposed method was finally integrated with a Robust Adaptive Unscented Kalman Filter (RAUKF) to track the dynamic states of the power system amidst uncertainties. The model, when experimented on an IEEE New England 10-generator 39-bus simulation system, could effectively bind uncertainties and improve estimation efficiency relatively. This survey was recommendable in testing the model with real-time plant, but it was rather complex with hybrid models.

Xiao et al., 2020 developed a mathematical model to describe the dynamic characteristics of a Medium-Voltage Integrated Power System (MIPS) for use in the dynamic State Estimation of a large marine power supply system. The model was based on the power systems network structure and control strategy. MIPS is a carefully coupled AC/DC hybrid power supply system proposed for large marine transport systems. Periodic disturbances caused by Pulse loads affect the accuracy of the dynamic state estimation and development of the power system as well as the filter stability. As the linearized mathematical model is less accurate during abrupt changes in the process dynamics, an Extended Kalman Filter (EKF) model was proposed to overcome these algebraic variables constraints during the State Estimation. Simulation results showed that the dynamic changes in the electro-mechanical transients and fault conditions were suppressed, thereby retaining filter stability. The mathematical model, when verified using a Gas Turbine and a Diesel Generator in real-time, produced closely similar results with permissible transient errors. This approach is limited in larger systems due to computational efficiency.

Zeng et al., 2019 proposed gas turbine parameter optimization using Unscented Kalman Filter (UKF) to first estimate some measured parameters as they change in operating points. A Particle Filter (PF) was also used to diagnose the different parameter performance by checking their health conditions to ascertain uninterruptible turbine operations. The simulation results yielded good performance. A single model would have done the same task of UKF and PF. This was rather computationally costly.

Cao et al., 2018 applied Model Predictive Control (MPC) model for gas turbine inlet temperature regulation. They proposed a control strategy based on Recurrent Neural Networks (RNN) to model the GT dynamics and implement the MPC algorithm. The experimental results, though proved effective work, was an expensive research work if implemented in real time.

Impraimakis and Smyth, 2022 examined the state estimation of an unknown input parameter using an Unscented Kalman Filter (UKF) on both linear and nonlinear systems. They used the system parameters to first predict the state of the dynamic system. In the second step, they used the system parameters again with the measurements to provide the final estimate of the input parameter. Perturbation Analysis was used to demonstrate this input parameter identification. The Analysis permits the unique identification of a system with a known input parameter either with a zero or non-zero value. The result was that all the dynamic states, parameters and inputs were jointly estimated in real time when compared to the classical output-only parameter identification. It would be better to separate linear loops from nonlinear loops to ascertain accuracies.

El-Sehiemy et al. 2020 investigated accurate Parameter Identification method and State of Charge (SoC) estimation for Lion Lithium (Li-Ion) battery. They used nonlinear electrical equivalent circuit to model the Lithium battery in the state space. The estimation problem of battery parameters and SoC were formulated as optimal problem with single and

multiple objective frameworks. Battery voltage or SoC or combined, were objective functions to be optimized. Enhanced Sunflower Optimization Algorithm (ESFOA) based on reduction strategy was developed to solve the optimization problem. Numerical simulations and experimental implementation were carried out on a 40Ah Li-Ion battery and compared. The model produced relatively higher accuracy optimal battery parameters. This study was time-consuming and computationally costly.

Haji et al., 2020 aimed at stabilizing the speed and temperature of a GT around their set points irrespective of load variations. They proposed an Adaptive Model Predictive Control (AMPC) scheme with Online Parameter Estimation. A recursive algorithm was used to estimate the unknown parameters at a time step with reference to current measurements and previous parameters. The effectiveness of the AMPC was implemented on a V94.2 GT unit in a life plant in Damavand on a comparative approach with three other robust controllers namely; Model Predictive Controller (MPC), H_∞ and *μ-synthesis*. The comparison was based on reference tracking, state-space responses, disturbance rejection and adaptive capabilities. Results obtained showed that the proposed model had the most superior performance. The V94.2 GT power plant recorded reasonable improvements on stability, robustness and other control features. This survey, though implemented with real-time data, was prone to error due to the combination of speed and temperature control loops at the same time.

Ping et al., 2019 proposed a novel Distributed State Estimation (DSE) model of an AC-DC hybrid microgrid power network system. Their aim was to address the network uncertainty associated with the existing Centralized State Estimation model. The microgrid network structure comprised of two autonomous AC and DC subsystems in coordinated operation. The Lagrangian relation method was used to decouple the AC and DC microgrid networks prior to the network monitoring. The proposed model executed the State Estimation of the microgrid network system in three stages. The first State Estimation processes are

executed in the first and the third stages. The second stage handles non-linear transformation of intermediate variables of the sub-systems passed from the first stage. Simulation results indicated that the proposed model was more superior and efficient than the existing Centralized model. The State variables such as the AC and DC voltages, along with AC phase angle had minimal errors. This procedure was computationally costly.

Sudev et al., 2017 proposed the use of Particle Filter (PF) for state estimations of three parameters of a Wind Turbine. The parameters under investigation were Tower Top Displacement, Tower Stop Velocity and Rotor Speed, which is the most mandatory as it directly depends on the wind speed. The idea is to predict and control the Rotor speed during excess wind. Simulation results proved that the PF produced good estimates of the parameters which perfectly restrained the output power of the Wind Turbine along its nonlinear regions. This study failed to apply real-time plant data for its simulation. Plant stability may not be ascertained under such condition.

Yaghoubi et al., 2022 observed that the legacy Swarm and evolutionary optimization algorithms were becoming less efficient for Photo-voltaic (PV) systems Parameter Estimation due to the non-linearity and increased complication of the PV systems. They proposed a more efficient, high-level, problem-independent model for PV Parameter Identification based on the Salp Swarm Algorithm (SSA). The Modified Salp Swarm Algorithm (MSSA) was characterized and tested on three PV panels. Simulation results indicated that numerous process variables and other PV characteristics were identified with higher efficiency than the legacy SSA and other sundry models. The MSSA produced better optimization solution with a Root Mean Square Error (RMSE) reduced by 69%. This is a complex process, and therefore certain parameters may not be estimated in details.

Arastou et al., 2022 implemented the Improved Heffron-Phillips (IHP) model using a multi-stage Unscented Kalman Filter (UKF) for simultaneous State and Parameter Estimation

in power system. They observed that the Traditional Heffron-Phillips model was less accurate for small signal stability analysis and power systems tuning in smart grids. The IHP was a third-order Synchronous Generator with a first-order Automatic Voltage Regulator (AVR) having Reactive Power compensation, Power Supply Stabilizer (PSS), and Turbine Governor model. Parameter sensitivity analysis was used to specify each part of the parameters at different stages. The unknown and remote parameters of interest were Mechanical Torque, Load Angle, Field Voltage, etc. Meanwhile, they were also treated as States for easy identification. The entire procedure, when finally applied on a 160MVA, 10.5KV, 50Hz gas unit and compared to an ordinary UKF, yielded higher accuracy, speed and convergence. Despite its superiority, it is computationally costly and time-consuming. Major details could be lost during computation.

OEM's Model: The OEM model in review is from Asean Brown Boveri ABB. The ABB model equations are shown below.

$$TIT = A*TAT + (B_{12}*(Tk_1)^2 + B_{11}*Tk_1 + B_{10})*\pi + (B_{22}*(Tk_1)^2 + B_{21}*Tk_1 + B_{20})*\pi^2 + RH_{corr.} + C \quad (2.38)$$

Where;

$$RH_{corr.} = E_{12}*(Tk_1)^2*RH + E_{11}*Tk_1*RH + E_{10}*Tk_1 \quad (2.39)$$

$$\Pi = \frac{Pk.median(barg)}{P_{exh}^2.min(bara)} \quad (2.40)$$

$$TAT = \frac{TATav}{100}, \quad (2.41)$$

$$RH = \frac{RHmin}{100}, \quad (2.42)$$

$$Tk_1 = \frac{Tk_1 median}{10} \quad (2.43)$$

ABB Model Equations (NAOC, 2006)

Despite being accurate for the TIT measurement, it is not available for any application, engineering analysis or modification by third world Engineers. Other OEMs also follow suite regarding their own models. It is proprietary and hardly available. The parameters have not been fully defined.

2.7 Review of Gas Turbine Models.

According to (Jonathan et al., 2018), industrial heavy-duty gas turbines (HDGT) are specially designed gas turbines for power generation employed in critical industries such as power generation, oil and gas, process plants, aviation as well as domestic and other related industries. Gas Turbine engines include high and low compressors, driven by high and low turbines respectively (Kniat, 1977). Historically, these heavy-duty gas turbine frame types were defined by their output, firing temperature and pressure ratio (Ducker, 2015). Higher output and better efficiencies soon evolved from technology. A new turbine class was always born each time a manufacturer could improve upon the output and efficiency (Ducker, 2015). The following classes of heavy-duty gas turbines are available:

1. D and E – class turbines are in the range of (75 – 110) MW.

2. F-class turbines are in the range of (170 – 230) MW.

3. G-, H-, and J- frames, also called advanced class turbines, range from (275 -350) MW.

A few OEMs with different grades of GT are as listed below with their product names: Some OEMs also produce other models for aviation and space flights, though not listed here.

1. General Electric (United States)
   a. GE 7E.03 (E-class)
   b. GE 7F.03-.05 (F-class)
   c. GE 7AH.01 and .02 (Advanced-class)

2. Siemens Energy (Germany)
   a. SGT6-2000E (E-class)
   b. SGT6-5000F (F-class)
   c. SGT6-8000H (Advanced -class)

3. Mitsubishi Hitachi (Japan)

a. H-100 (E/D -class)

b. M501F, M701F4 (F-class)

c. M501J, M501G (Advanced -class).

4. Alstom Power (France)

a. GT13E2, GT11, GT12 (E – Class).

b. GT24, GT26 (F-Class).

5. Asean Brown Boveri - ABB Power (Switzerland)

a. GT 24, GT 26 (Advanced -class) (Ducker, 2015).

2.8 Research Gaps

It is a known fact that every measurement process is surrounded by uncertainties. A single measurement is contaminated with process and measurement noise signals in the form of normal or Gaussian distributions with probability density functions (pdf) similar to the measured parameter. To this end, every model under review is struggling to attenuate these covariance signals interfering with the measurements. Some scholars have developed additional algorithms to suppress the spurious signals before integrating them into their measurement models. In doing this, they arrive at hybrid models which become complex, computationally costly and time consuming. Some scholars on another hand chose to investigate an entire complex system comprising both linear and nonlinear control loops. Because of this, useful details are lost, leading to reduced accuracies. Majority of the scholars relied on arbitrary figures instead of Real-time process information. The model designed by ABB though efficient, is strictly proprietary, and somewhat not available to the growing Engineers. Apart from its complexity, it is computationally costly. Most of the Parameters used have not been defined in scientific terms, leaving the model as a mere black box that Engineers cannot understand. The ABB model cannot be reproduced or modified by the teaming Engineers in third world countries. The Research Gap is to separate linear loops from a nonlinear complex system and use the practical results obtained from ABB model to

characterize a known model and compare the two results. Parameter Estimation and noise signal filtering will be handled by a single model.

CHAPTER THREE

MATERIALS AND METHOD

3.1 Materials

Materials used for this research work are:

I. Real-Time Process Data from two identical Gas Turbines: GT11 and GT12 (Table 3.1).

II. Thermodynamics Temperature Equation.

III. Thermal Efficiency Model.

IV. Additional Parameters are theoretical Constants peculiar to gas and air.

V. MATLAB R2021a software.

VI. Intel Corei5, 2.5GHz, 6GB RAM HP Laptop.

3.2 Method

Table 3.1 contains all the process information obtained from the two identical 150MW Gas Turbines, namely, GT11 and GT12. The process information is first used with the thermodynamic Temperature Equation to theoretically compute the Inlet Temperatures for the two GTs using MATLAB Command window. Adiabatic Efficiency is an important parameter that must be derived theoretically from other process variables. After these computations, the System Matrices are generated for the Kalman Filter simulation. MATLAB Codes will then be generated to make the simulations feasible. Thermal energy is calculated for the two GTs, and compared with the plant data. Then all the computed values of the TIT ($T3$) will be compared with the given Temperature data from GT11 and GT12. Process Noise covariance signals are introduced into the Filter while observing its filtering capability.

3.2.1 Real-Time Process Data from IPP, Okpai

Table 3.1 contains all the information from the two identical Gas Turbines as deduced from Plates 2 and 3 of Appendix A. They will be used to derive the unknown parameters needed for the modelling as follows.

Table 3.1 Process Data from Independent Power Plant, Okpai (NAOC, 2024).

S/N	Parameter	Sym	GT11	GT12	Unit
1	Compressor Inlet Temperature	*T1*	30.16	31.0	^{O}C
2	Temperature After Compressor	*T2*	410	369	^{O}C
3	Compressor Inlet Pressure	*P1*	1002	1000	mbar
4	Compressor Discharge Pressure	*P2*	13.5	9.7	Bar
5	Fuel Gas Flow Rate	*mf*	8.68	4.36	Kg/s
6	Turbine Inlet Temperature	*T3*	1110	780	^{O}C
7	Temperature After Turbine	*T4*	533	366	^{O}C
8	Output Power	P_E	145	40	MW
9	Lower Heating Value	*Hv*	39.60	39.60	MJ/Nm^3
10	Fuel-to-Air Ratio	*F*	0.031	0.028	-
11	Specific Heat Coefficient of Air	*cp*	1.005	1.005	KJ/kg*K

3.2.1.1 Calculations from GT11 Process Data

From Table 3.1, the following parameters shall be used in calculating other unknown parameters needed for the system.

P1 = 1002; *% Compressor Inlet Pressure (mbar)*

P2 = 13.5; *% Compressor Discharge Pressure (bar)*

T2 = 410; *% Temperature After Compressor (^{o}C)*

mf = 8.68; *% Fuel Gas Mass Flow Rate (kgs^{-1})*

f = (*mf*/*ma*) = 1:32; *% Fuel-To-Air Ratio* (3.1)

ma = (8.68 X 32) = 277.760; *% Air Mass flow (kgs^{-1})*

Hv = 3.9600000; *% Fuel Gas Heating Value (MJ/Nm^3)*

cp = 1.005; *% Specific Heat Capacity of Air (KJ/kg*K)*

γ = 1.4. *% Adiabatic Index*

(a). Thermal Efficiency for GT11.

The Thermal Efficiency (η_t) for GT11 can be computed from the plant data using the Pressure Ratio, *P2/P1* and Adiabatic Index, (γ) as follows:

$$\eta_t = 1 - \frac{1}{[P2/P1]^{(\gamma - \frac{1}{\gamma})}} \quad \textit{(Proctor II, 2003)} \qquad (3.2)$$

$$\eta_t = 1 - \frac{1}{[13.5/1.002]^{(1.4 - \frac{1}{1.4})}} \quad \textit{\% Substituting for P1, P2 and } \gamma,$$

$$\eta_t = 1 - \frac{1}{[13.473]^{(0.686)}} \quad \textit{\% solving individual brackets,}$$

$$\eta_t = 1 - \frac{1}{5.954} \quad \textit{\% removing the brackets,}$$

η_t = 0.83 ≈ 83% *% final value for thermal efficiency.*

(b). Thermal Energy for GT11

The Thermal Energy (*Eth*) for GT11 using MATLAB Code:

Eth = (*mf* * *Hv* * η_t) (3.3)

```
>> mf = 8680;                    % Fuel Gas Mass Flow Rate
>> Hv = 39600000;                % lower Heating Value of Fuel Gas
>> ηt = 0.83;                    % Thermal Efficiency
>> Eth = (mf*Hv*ηt)              % From equation (3.3), Thermal Energy,
Eth =
  2.8530e+11 Joules             % Eth in engineering units.
```

= 285GJ.

3.2.1.2 Calculations from GT12 Process Data

From Table 3.1 also, the following input parameters shall be used to calculate some unknown parameters for GT12.

P1 = 1000; *% Compressor Inlet Pressure (mbar)*

P2 = 9.7; *% Compressor Discharge Pressure (bar)*

T2 = 369; *% Temperature After Compressor (^oC)*

mf = 4.36; *% Fuel Gas Mass Flow Rate (kgs^{-1})*

f = (*mf/ma*) = 1:36; *% Fuel-To-Air Ratio*

ma = (4.36 X 36) = 156.960; *% Air Mass flow (kgs^{-1})*

Hv = 39.600000; *% Fuel Gas Heating Value (MJ/Nm^3)*

cp = 1.005; *% Specific Heat Capacity of Air (KJ/kg*K)*

Υ = 1.4 *% Adiabatic Index*

(a) Thermal Efficiency for GT12

The Thermal Efficiency (η_t) is also calculated using Pressure Ratio, *P1/P2* for GT12 and Adiabatic Index, (Υ) as follows:

From eqn. (3.2),

$\eta_t = 1 - \frac{1}{[P2/P1]^{(\gamma - \frac{1}{\gamma})}}$ (*Proctor II, 2003*)

$\eta_t = 1 - \frac{1}{[9.7/1.000]^{(1.4 - \frac{1}{1.4})}}$ *% Substituting for P1, P2 and Υ,*

$\eta_t = 1 - \frac{1}{[9.70]^{(0.686)}}$ *% solving individual brackets,*

$\eta_t = 1 - \frac{1}{4.753}$ *% removing the brackets,*

η_t = 079. ≈ 79% *% final value for thermal efficiency.*

(b) Thermal Energy for GT12

From eqn. (3.3), the Thermal Energy (*Eth*) for GT11 using MATLAB Code:

Eth = ($mf * Hv * \eta_t$)

```
>> mf = 4360;                          % Fuel Gas Mass Flow Rate
>> Hv = 39600000;                      % lower Heating Value of Fuel Gas
>> ηt = 0.79;                          % Thermal Efficiency
>> Eth = (mf*Hv*ηt)                    % From equation (3.3), Thermal energy,
Eth =
   1.3640e+11 Joules                   % Eth in engineering units.
```

= 136 GJ.

3.2.2 Computation of Burner Can Temperature Rise Equation

From the empirical thermodynamics "burner can temperature rise'' equation, fuel-to-air ratio is given by:

$$f = \frac{\left(\frac{T3}{T2}\right)-1}{\left(\frac{\eta tHv}{cpT2}\right)-\left(\frac{T3}{T2}\right)} \qquad (NASA,\ 2021) \qquad (3.4)$$

$f = \frac{\left(\frac{T3-T2}{T2}\right)}{\left(\frac{\eta tHv-cpT3}{cpT2}\right)}$ % regularizing equation (3.4),

$f = \left(\frac{T3-T2}{T2}\right)$ x $\left(\frac{cpT2}{\eta tHv-cpT3}\right)$ % separating the two major fractions,

$f = \left(\frac{cpT2(T3-T2)}{T2(\eta tHv-cpT3)}\right)$ % multiplying out the brackets,

$f = \left(\frac{cp(T3-T2)}{(\eta tHv-cpT3)}\right)$ % dividing through by T2, (3.5)

$\eta tHvf - cpT3f = cpT3 - cpT2$ % cross multiplying equation (3.5),

$-cpT3f - cpT3 = -cpT2 - \eta tHvf$ % collecting terms in T3,

$-(cpT3f + cpT3) = -(cpT2 + \eta tHvf)$ % factorizing the terms again,

$T3 = \left(\frac{cpT2+\eta tHvf}{cpf+cp)}\right)$ % making T3 the subject formula,

$T3 = \left(\frac{cpT2+\eta tHvf}{cp(1+f)}\right)$ % T3 finally derived thus: (3.6)

3.2.2.1 Theoretical Computation of *T3* for GT11 Plant Model.

$T3 = \left(\frac{cpT2+\eta tHvf}{cp(1+f)}\right)$ *% from equation 3.6,*

Solving directly for *T3* from the burner can temperature rise equation above, and substituting the values for the GT Parameters using MATLAB Code, the following computation is obtained:

```
>> cp = [1005];                    % specific heat capacity of air
>> T2 = [410];                     % compressor discharge temperature
>> η_t = [0.83];                   % thermal efficiency for GT11 Model
>> Hv = [39600000];                % lower heating value of fuel gas,
>> mf = [8680];                    % fuel gas flow rate,
>> ma = (mf*32)                    % air mass flow rate,
 ma =     277760                   % calculated air mass flow,
>> f = (mf/ma)                     % fuel to air ratio,
f =       0.0312                   % f is unitless.
>> den = (cp*(1+ f))               % expression for the denominator,
den =   1.0364e+03                 % denominator is approximately:
>> num = (cp*T2) +( η_t*Hv*f)      % expression for the numerator,
num =   1.4392e+06                 % numerator is approximately:
>> T3 = (num/den)                  % T3 is (numerator/denominator)
T3 =   1.3886e+03                  % T3 in engineering units
```

T3 ≈ 1,388°C *% T3 for GT11 is approximately,*

3.2.2.2 Theoretical Computation of *T3* for GT12 Plant Model

Computing *T3* using MATLAB Code,

```
>> cp = [1005];                    % Specific Heat Capacity of Air,
```

```
>> T2 = [369];                          % Compressor Discharge Temperature,

>> ηt = [0.79];                         % Thermal Efficiency for GT11 Model

>> Hv = [39600000];                     % lower Heating Value of Fuel Gas,

>> mf = [4360];                         % Fuel Gas Flow Rate,

>> ma = (mf *36)                        % Air Mass Flow Rate,

 ma =      156960                       % Calculated Air Mass Flow,

>> f = (mf/ma)                          % Fuel-To-Air Ratio,

f =    0.0278                          % f is unitless.

>> den = (cp*(1+ f))                    % expression for the denominator,

den =    1.0329e+03                     % the denominator is approximately,

>> num = (cp*T2) +( ηt*Hv*f )           % expression for the numerator,

num =    1.2399e+06                     % the numerator is approximately,

>> T3 = (num/den)                       % T3 is (numerator/denominator),

T3 =    1.2003e+03                     % T3 in engineering units

T3 ≈     1,200°C                        % T3 for GT12 is approximately,
```

3.2.3 Characterization of the Kalman Filter Model.

This involves the generation of configuration parameters for the plants and the filter model in the State Space before simulations.

3.2.3.1 Generating System Matrices

Defining the State variables;

$x1 = T2,$ (3.7)

$x2 = T3,$ (3.8)

Deriving the equations that relate the state variables to the inputs and output of the system using Energy Balance Equation:

$mfHv = maCp\ (T3 - T2)$ (3.9)

$mfHv = maCp\ (x2 - x1)$ *% substituting for T3 and T2,* (3.10)

$T3 = \left(\frac{Cpx1+\eta tHvf}{Cp(1+f)}\right)$ *% from equation (3.6),*

To put this equation into state space form, it is first expressed in terms of state variables and inputs.

$mfHv = maCp\ (x2 - x1)$ *% solving for x2 in equation (3.10),*

$mfHv = maCpx2 - maCpx1$ *% removing the bracket,*

$maCpx2 = mfHv + maCpx1$ *% separating the term in x2,*

$x2 = \frac{mfHv+macpx1}{macp}$ *% making x2 the subject formular,*

$x2 = \frac{mfHv}{macp} + x1$ *% separating the numerator,* (3.11)

In state space form the following equations are obtained:

$x1\_dot = 0$ (3.12)

$x2\_dot = \frac{mfHv}{maCp} - \frac{x2(1+f)}{Cp(1+f)z}$ (3.13)

where;

$z = \frac{maCp}{mfHv}$ *% z is a constant* (3.14)

The input and output equations are:

$u = f$ (3.15)

y = *T3* (3.16)

Re: $x1\_dot = Ax + B\text{u}$

$\text{y} = Cx + D\text{u}$

$$\text{A} = \begin{bmatrix} 0, & 0 \\ 0, & \frac{-(1+f)}{cp(1+f)z} \end{bmatrix};$$

B = [0; 1];

C = [0, 1];

D = [0]

(a) System Matrices for GT11

A = [0, 0;0, -0.00087998844459618209]

B = [0; 1]

C = [0, 1]

D = [0]

(b) System Matrices for GT12

A = [0, 0;0, -0.0012445291122439807]

B = [0; 1]

C = [0, 1]

D = [0]

3.2.3.2 Introducing Noise Covariance Signals into the Systems.

Process noise matrix depends on the number of states. For the 2 states, the process noise will have a 2x2 identity (I) matrix to be multiplied with the Process Noise Variance (PNV). The

measurement noise matrix on the other hand depends on the number of outputs. In this case, the measurement noise will have a 1x1 identity for its computation since *T3* is the only output.

(a) Process Noise for GT11 Plant Model

$PNstd = 0.002;$ *% Process Noise Standard Deviation,*

$PNV = PNStd\text{^}2 = 0.0004$ *% PNV is Process Noise Variance,*

$I = \begin{matrix} 1 & 0 \\ 0 & 1 \end{matrix}$ *% I is a 2x2 Identity Matrix,*

$Q = I * PNV$ *% Q is Process Noise Covariance* (3.17)

$= \begin{matrix} 0.0004 & 0.0000 \\ 0.0000 & 0.0004 \end{matrix}$ *% Matrix.*

(b) Measurement Noise for GT11 Plant Model

$MNstd = 0.05;$ *% Measurement Noise Standard Deviation,*

$MNV = MNStd\text{^}2 = 0.0025$ *% MNV is Measurement Noise Variance,*

$I = [1]$ *% I is a unit Matrix,*

$R = I * MNV$ *% R is Measurement Noise* (3.18)

$= 2.5e-03$ *% Covariance Matrix.*

(c) Process Noise for GT12 Plant Model

$PNstd = 0.06;$ *% Process Noise Standard Deviation,*

$PNV = PNStd\text{^}2 = 0.0036$ *% PNV is Process Noise Variance*,

$I = \begin{matrix} 1 & 0 \\ 0 & 1 \end{matrix}$ *% I is a 2x2 Identity Matrix,*

$Q = I * PNV$ *% From (3.16), Process Noise Covariance*

$= \begin{matrix} 0.0036 & 0.0000 \\ 0.0000 & 0.0036 \end{matrix}$ *% Matrix (Q).*

(d) Measurement Noise for GT12 Plant Model

$MNstd = 0.05;$ *% Measurement Noise Standard Deviation,*

$MNV = MNStd\text{^}2 = 0.0025$ *% MNV is Measurement Noise Variance,*

$I = [1]$ *% I is a unit Matrix,*

$R = I * MNV$ *% From (3.17), R is Measurement Noise*

$= 2.5e-03$ *% Covariance Matrix.*

3.2.4 Simulation of the Kalman Filter Model

The following blocks are used for the simulation.

I. Constant block.

The Constant block is a commonly used SIMULINK block. It will be used to configure constant values for input parameters. In this application, it will generate real constant signal values in matrix form for all the A, B, C Parameters representing the process plant.

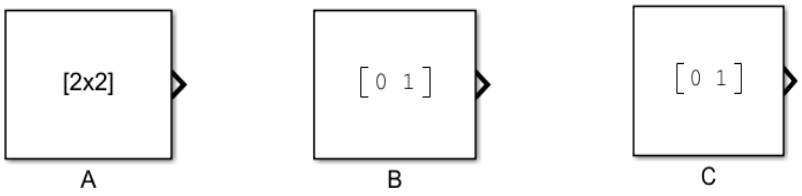

II. Signal Delay block

The Delay block delays the input signal by a specified number of samples before transmitting it to the next block. The Sample Time is 0.01seconds, with initial condition of 0.0, and delay length of 1.0.

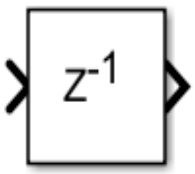

III. Matrix Multiply block

The Matrix Multiply block is used to multiply the input matrix elements. The number of rows and columns for matrix multiplication must agree before this operation is done.

IV. Summing block

The Summing block will be used to add the product of the input parameters together, and also to introduce the spurious noise signals into the System at different stages of the plant operation.

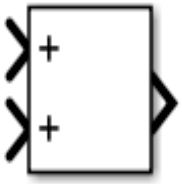

V. Random Signal block

The Random Signal block is used to output a normally Gaussian distributed process and measurement noise signals. This block will compute the Variances of the different noise signals with a sampling time of 0.01 seconds.

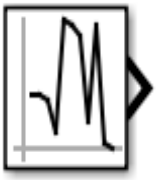

VI. Kalman Filter block

The Kalman Filter block is the main Controller that will estimate the Inlet Temperature of the Gas Turbines in discrete time domain. It is configured using the A, B, C, D Parameters obtained from the Plant Model as well as the Process and Measurement Noise Characteristics intentionally introduced into the system. The input vector from the Plant is connected to

terminal u, while the output of the Plant is connected to terminal y of the Kalman filter. The estimated state of the Model is obtained as xhat.

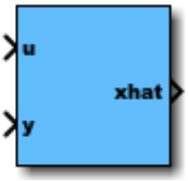

VII. Scope

The Scope is used to display signals generated during simulations. The noise signals and the estimated temperature are displayed on the scope at different points.

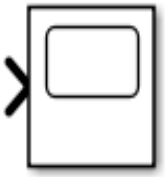

VIII. The SIMULINK Model

The SIMULINK Model is an interconnection of all the process blocks with the Kalman Filter block. The process blocks constitute the plant model, while the Kalman Filter block represents the Controller model.

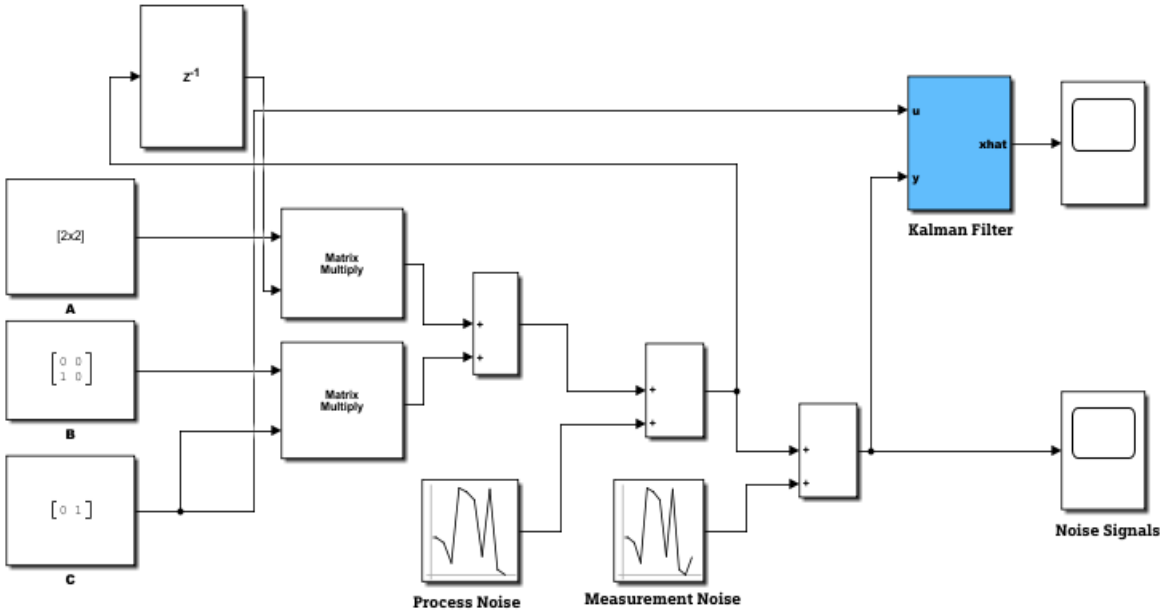

Fig. 3.1: SIMULINK Model for Kalman Filter Implementation (I Love MATLAB, 2020).

CHAPTER FOUR

RESULTS AND DISCUSSION

4.1 Results

The Kalman Filter model was characterized in Discrete Time using the earlier derived A, B, C, D Parameters from the GTs along with Noise Covariance signals as shown in figure 4.1. Other Parameters used for the configuration are Process Noise (Q) and Measurement noise (R) characteristics.

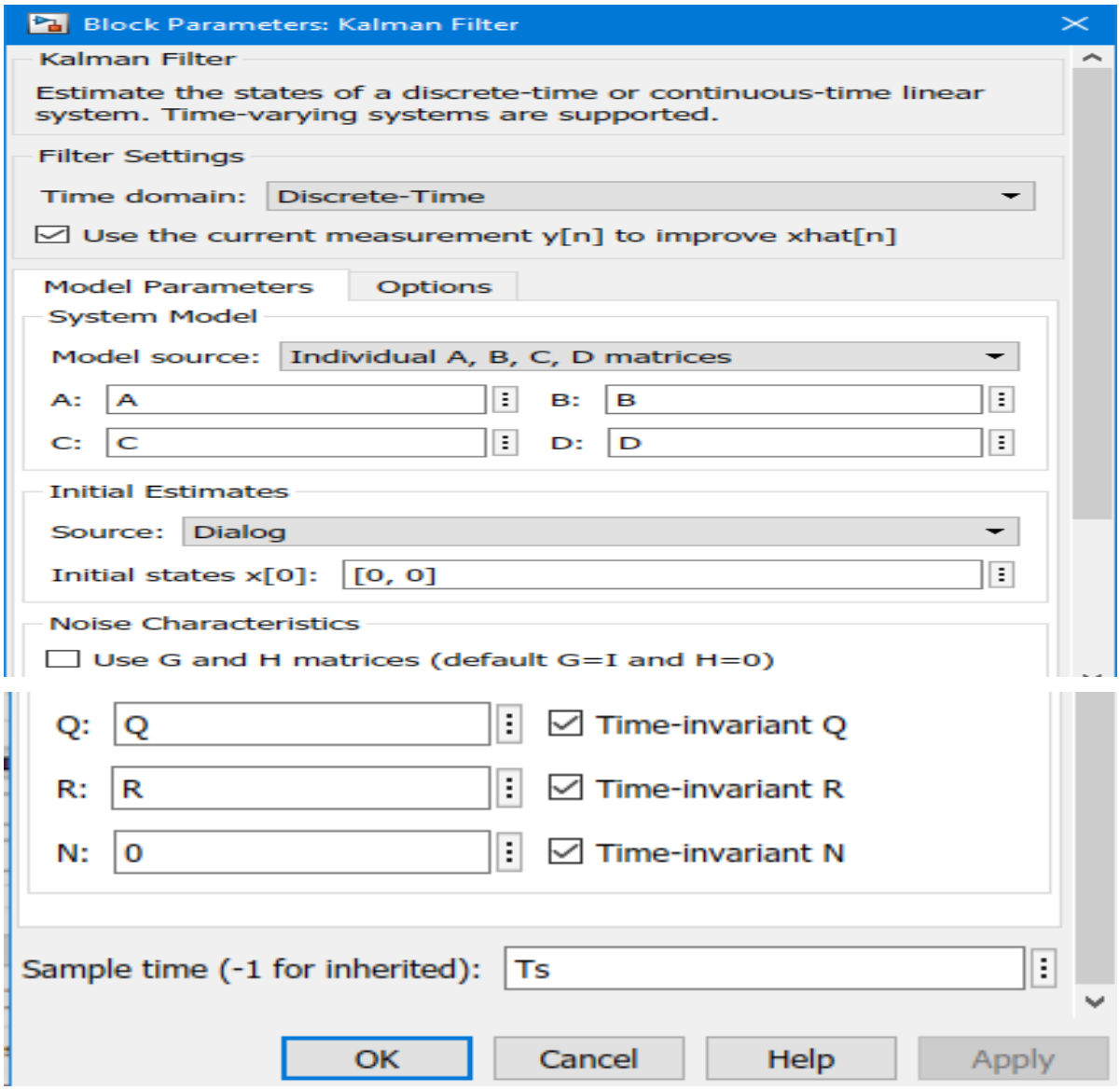

Fig. 4.1: Characterization of the Kalman Filter Model

4.1.1 Turbine Inlet Temperature Plot for GT11 Model.

Figure 4.2 is a State Space model showing the Gas Turbine Inlet Temperature (TIT) Estimation for GT11 plant model. The estimated temperature value is 1130^{0}C (brown), while the noise (N) signal is negligible along the X-axis (blue).

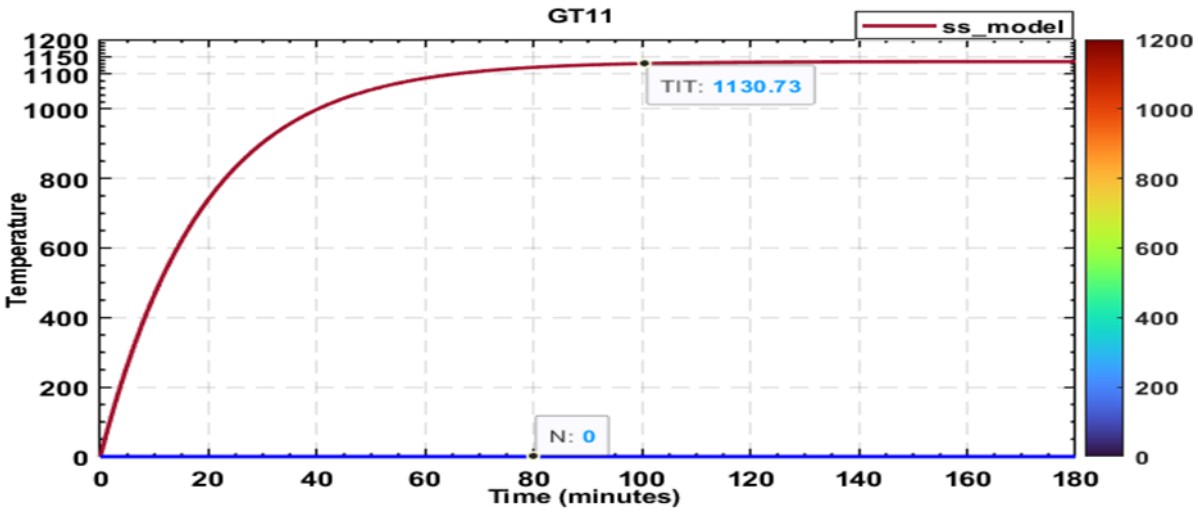

Fig. 4.2: Estimated Temperature Plot for GT11 Model

4.1.2 Unprocessed Noise Signals for GT11 Model

Figure 4.3 is a plot showing the fictitious noise signals superimposed into the plant model before the filter action. The Measurement and Process Noise signals are represented as blue and yellow colours respectively.

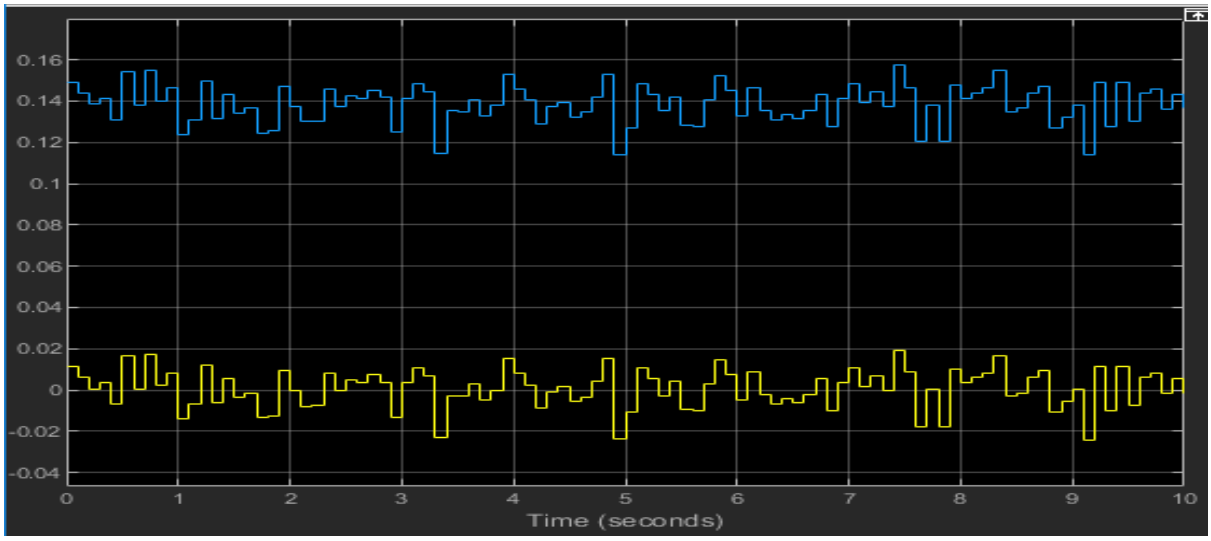

Fig. 4.3: Unfiltered Noise Signals for GT11 Model

4.1.3 Processed Noise Signals for GT11 Model

Figure 4.4 is a plot of the two noise signals for GT11 plant model being properly filtered and decoupled from the estimated temperature. The Measurement Noise (brown) is always higher than the Process Noise (blue).

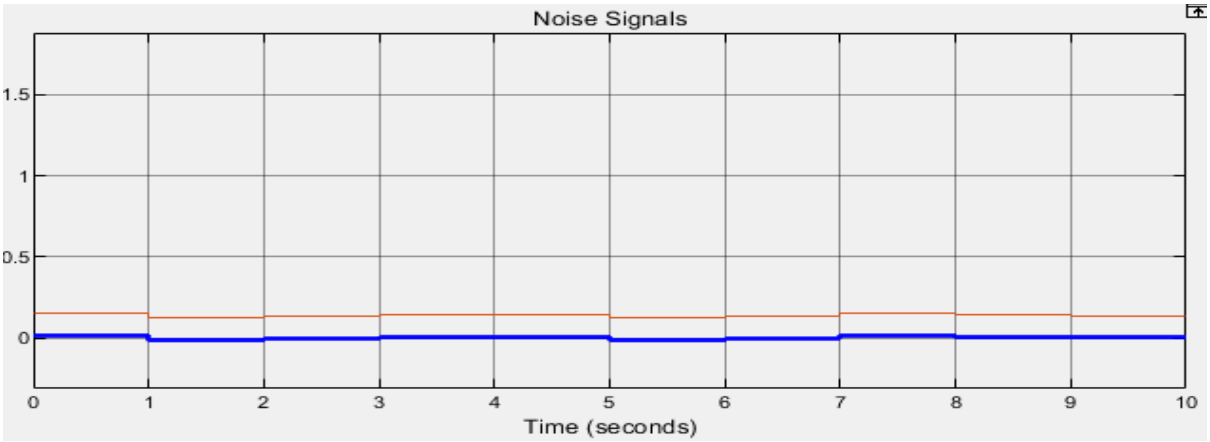

Fig 4.4: Filtered Noise Signals for GT11 Model

4.1.4 Filter Gain and Positive Definite Matrix for GT11 Model.

K = (2x2)

0.5370 -0.4630

-0.4630 0.5370

P = (2x2)

0.0001852 0.0001852

0.0001852 0.0001852

4.1.5 Turbine Inlet Temperature Plot for GT12 Model.

Figure 4.5 is the State Space model plot for GT12 Estimated Temperature. The Turbine Inlet Temperature estimate is 801.49^{0}C as clearly indicated on figure 4.5. Here again the Noise signals (N) have been filtered from the measurement and relegated to the background along the X-axis.

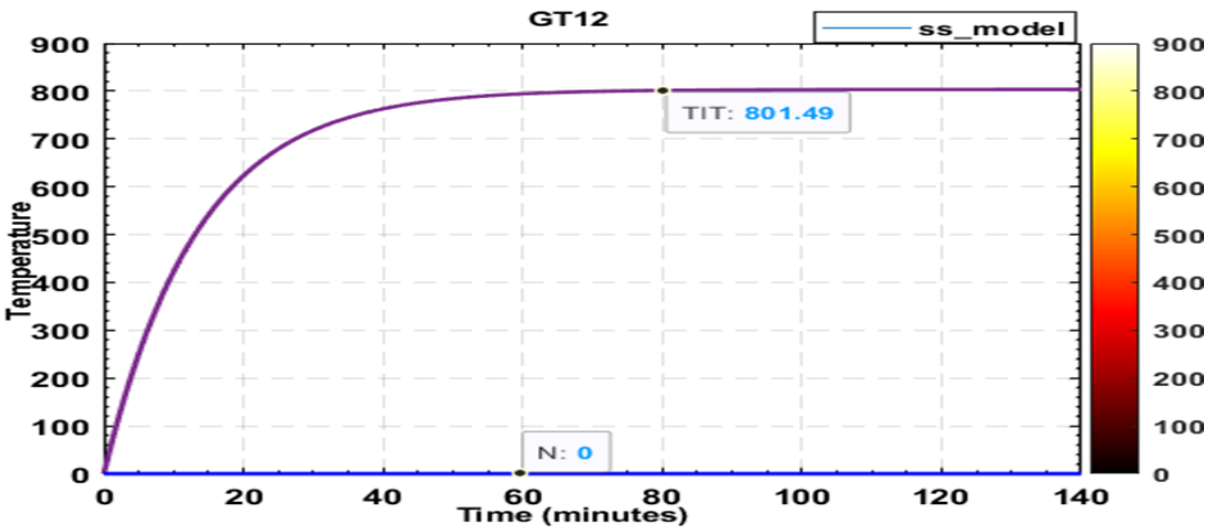

Fig. 4.5: Estimated Temperature Plot for GT12 Model

4.1.6 Unprocessed Noise Signals for GT12 Model

Figure 4.6 is a plot showing Process Noise (blue) and Measurement Noise (yellow) for GT12 plant model. The plot indicates that the noise signals have not yet been filtered by the KF model.

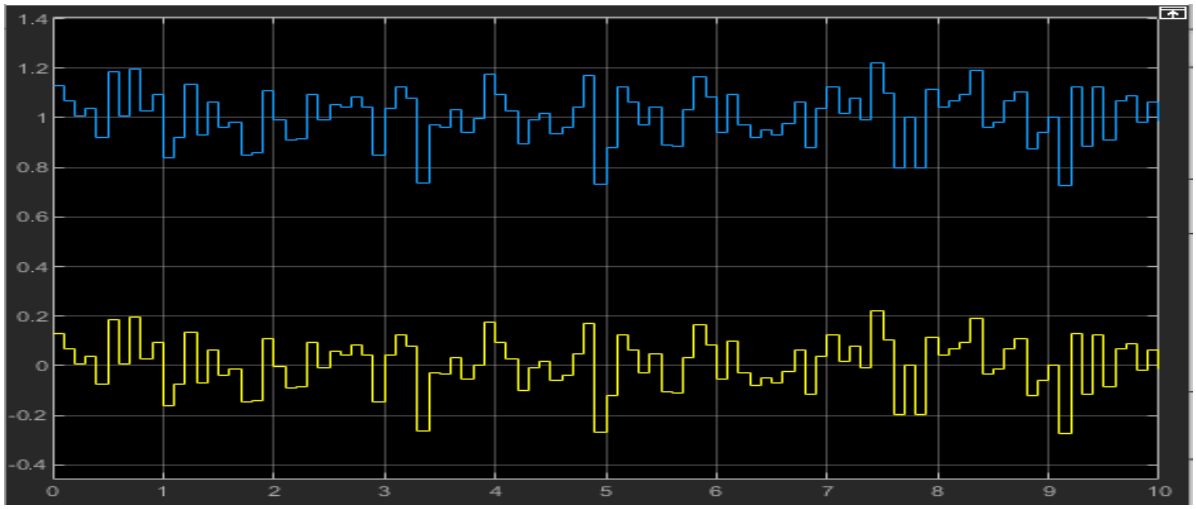

Fig. 4.6: Unfiltered Noise Signals for GT12 Model

4.1.7 Processed Noise Signals for GT12 Model

Figure 4.7 is a plot of the Process and Measurement Noise signals for GT12 plant model after the Kalman Filter action.

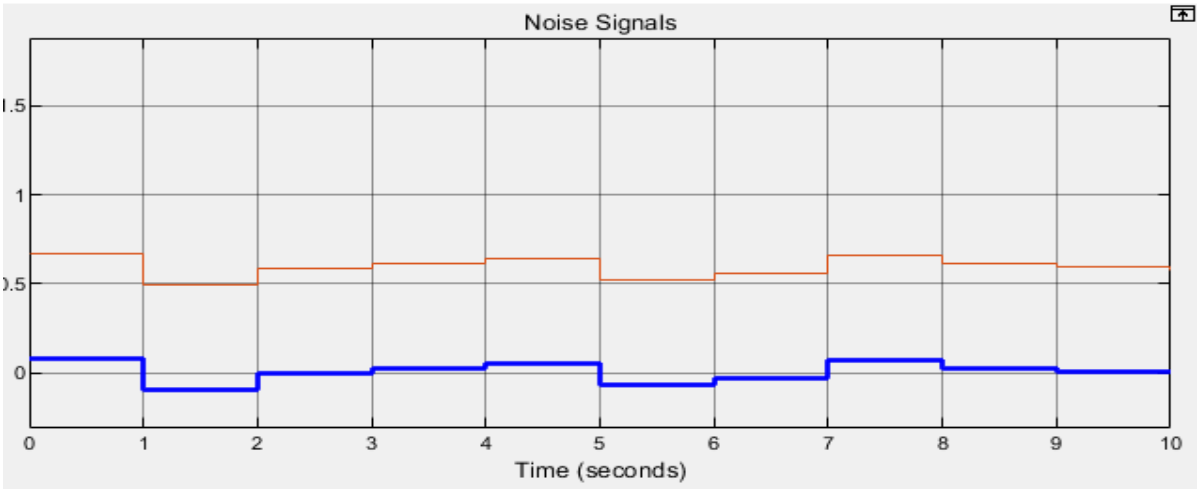

Fig. 4.7: Filtered Noise Signals for GT12 Model

4.1.8 Filter Gain and Positive Definite Matrix for GT12 Model.

K = (2x2)

0.7093 -0.2907

-0.2907 0.7093

P = (2x2)

0.0010 0.0010

0.0010 0.0010

4.1.9 Validation of the Kalman Filter Model

Table 4.1 is a validation Table for the Kalman Filter model. It presents the numeric values obtaind from the simulations and from theoretical values in a comparative approach. From Table 3.1, the standard Plant values of *T3* for comparison are 1110°C and 780°C for GT11 and GT12 respectively.

Table 4.1: Validation Table for Kalman Filter and Calculated values.

Model Plant	GT11(°C)	%Accuracy	GT12 (°C)	%Accuracy
Calculated Values	1388	80	1200	65
Simulated Values	1130.73	98.1	801.49	97.2

4.2 Discussions

Theoretical computations of the GT Inlet Temperature produced 80% and 65% accuracies for GT11 and GT12 plant models respectively. This suggests that ordinary calculation alone cannot sufficiently estimate the unknown States of the turbulent Gas Turbine system. The noise factors cannot be addressed with the ordinary Thermodynamic Temperature equation.

Simulation results from the Kalman Filter model have shown great improvements. As obtained in Table 4.1, the model achieved 98.1% and 97.2% accuracies for GT11 and GT12 respectively. Achieving this great feat was made possible by manipulating the Fuel-to-Air Ratios. In GT11, the Ratio was adjusted to 1:32; while in GT12, the Ratio was maintained at 1:36. This Fuel-to-Air Ratios mean that more fuel was injected into GT11, while more air was injected into GT12 due to higher load demand for GT11. During simulations, the Filter model automatically generated its Gain (K) as well as the Positive Definite Matrix (P) needed for smooth prediction and filtering respectively. Temperature estimates attained stability at 100min and 80min for GT11 and GT12 respectively. This further confirms that the more the filtering capability, the more the time taken to attain stability. The unwanted signal frequencies were decoupled from the measurement earlier, and suppressed along the X-axis (time) in blue colour, as illustrated in Figure 4.2 and Figure 4.5 for GT11 and GT12 respectively. It was realised that the higher the noise, the higher the values of K and P. Since more Noise signals were introduced into GT12 than GT11, the K and P matrices were higher in values for GT12 than for GT11. Figure 4.3 and Figure 4.6 represent the early stages of the Noise signals, while Figure 4.4 and Figure 4.7 illustrate their conditions after filtration.

CHAPTER FIVE

CONCLUSION AND RECOMMENDATIONS

5.1 Conclusion:

The research objectives have been fulfilled. Real-time process data was collected from two running plants and used for the modelling. A simpler thermodynamic temperature equation was used to generate the system matrices in the state space for the internal combustion engine. Certain plant parameters had to be determined based on theoretical inferences for successful modelling. Those parameters are Fuel–to– Air ratio, Specific Heat Ratio of Air, Adiabatic Index and Adiabatic Efficiency of the Compressor. To achieve accurate estimates, some trade-offs had to be performed among the parameters. This model does not involve the Temperature After Turbine (*T2*) as one of its input signals, compared to the proprietary model used by ABB for the power plant. All forms of noise covariance signals from the process and measurement data have been successfully filtered during the measurement. The essence of obtaining two sets of plant data from GT11 and GT12 was to check the filter performance on two different occasions. The Kalman Filter has responded accurately during fuel gas increase along with Compressor Discharge Temperature variations. The use of Kalman Filter model with real-time process data for estimation of Gas Turbine Inlet Temperature has been validated. In earnest, Kalman Filter characterization might be the immediate contender in Gas Turbine and other process Parameter Estimations in the industry due to its simplicity and accuracy.

5.2 Recommendations.

i. Optimizing Inlet Temperature Estimation through Loop Tuning

To improve the responsiveness and accuracy of the Inlet Temperature Estimation, it is recommended to perform software loop tuning. Further optimization is necessary to reduce the

response time of the system and enhance real-time performance. This improvement can be achieved through:

- Fine-tuning control loop parameters to better match the plant dynamics.
- Introducing additional poles to the process model in continuous time, if necessary, to refine system behaviour and stability.

By addressing these aspects, the estimation process can become faster and more reliable, supporting more effective decision-making in real-time operations.

ii. Evaluating Alternative Kalman Filter Models with Plant Data

To enhance the reliability and accuracy of real-time plant data estimation, it is recommended to test the dataset using alternative Kalman filter models. Specifically, the Extended Kalman Filter (EKF), Unscented Kalman Filter (UKF), and Particle Filter (PF) should be implemented and evaluated. These models should be applied in a manner consistent with the current methodology to ensure a fair comparison. The goal is to assess and compare the performance of each filter in real-life plant scenarios, focusing on accuracy, robustness, and computational efficiency. This comparison can inform the selection of the most suitable filtering approach for future implementations in dynamic plant environments.

5.3 Contributions to Knowledge.

This research work has successfully made the following contributions to the body of knowledge. It has successfully derived System Matrices from a linear temperature equation, making it compatible for integration with a Kalman Filter model. This advancement enables the utilization of an open-source Kalman Filter for Gas Turbine temperature measurements, particularly beneficial for developing countries. Key highlights of these contributions include:

i. **Innovative Development:** The research introduces a method for constructing system matrices that enhances the functionality of Kalman Filter models in remote temperature measurement applications.

ii. **Accessibility:** By leveraging an open-source framework, the model allows developing countries to implement and adapt advanced temperature measurement technologies without the constraints of proprietary software.

iii. **Real-Time Application:** The revised model is now capable of performing effectively in real-time scenarios, comparable to existing closed-source models, thus providing practitioners with a viable alternative for temperature monitoring in Gas Turbines and other internal combustion engines.

iv. **Potential for Future Advancements:** This work lays the groundwork for further modifications and technological advancements, promoting ongoing development in the field.

REFERENCES

Aakash-JEE. (2021). *Concept of the Day: Adiabatic Process*. Retrieved from Adiabatic Process Derivation - BYJU'S: https://byjus.com

ABB. (2024). *Introduction to Advanced Process Control (APC) Solutions.* Retrieved from Advanced Process Control Software: https://new.abb.com

Ahmed, R. (2023). "Optimization and State Estimation Fundamentals". Udemy Inc Online Lessons.

Aminov, R. Z., & Moskalenko, A. B. (2018). "Optimal Gas Turbine Inlet Temperature for Cyclic Operation". *Journal of Physics Conference Series.* IOP Publishing.

Antai, L. and Chen, J. (2023). *"Normal Distribution".* Dotdash Meredith, Investopedia.com.

Arastou, A., Rabieyan, H., Karrari, M. and Hosseini, S. M. (2022). "Dynamic State and Parameter Estimation of the Improved Heffron-Phillips using a Fast UKF-Based Algorithm and a Novel Rotor Angle Measurement Approach". *Electric Power Systems Research: Researchgate*.

Asgari, H. (2014, February). "Modelling, Simulation and Control of Gas Turbines Using Artificial Neural Networks". University of Canterbury, Christchurch, New Zealand.

Augustyn, A. (2023). *"Gaussian Noise".* Retrieved from Encyclopaedia Britannica: https://en.wikipedia.org.

Basu, S. and Debnath, K. (2019). "Turbine Firing Temperature". *Power Plant Instrumentation & Control Handbook, 2nd Edition*.

Battista, R. A., Pandalai, R. P. and Hilt, M. B. (1982). *"Low Heating Value Fuel Burning Capabilities of General Electric Industrial Gas Turbines".* Retrieved from The American Society of Mechanical Engineers (New York).: http://asmedigitalcollection.asme.org/GT/proceedings-pdf/GT

Biezen, M. V. (2015). *"The Kalman Filter: The Multi-Dimension Model 1".* . Retrieved from http://ilectureonline.com.

Biswas, D. (2024, July 10). *"Gas Turbine Systems and Instrumentation".* Retrieved from Linkedin: www.linkedin.com

Boyce, M. P. (2006). "Gas Turbine Engineering Handbook". . Gulf Professional Publishing, 3rd Edition.

Boyce, M. P. (2012). "An Overview of Gas Turbines". *Science Direct: Elservier*.

Brooks, F. J. (2010). "GE Gas Turbine Performance Characteristics". *GER-3567H.* Schenectady, New York, U.S.A: GE Vernova.

Bruce, G. M. (2011). "Clean Coal Technologies for Advanced Power Generation." . *Science Direct Journals and Books.*

Burnes, D. and Camon, A. (2019). "Impact of fuel composition on Gas Turbine Engine Performance". . *Journal of Engineering for Gas Turbines and Power.*, 141(10).

Cao, Y., Yang, C and Li, C. (2018). “Model Predictive Control of Gas Turbine Inlet Temperature Based on Recurrent Neural Networks". *Journal of Energy Engineering.*

CSA. (2013). “Air Fuel Ratio of the Gas Turbine". Control.com.

Dasgupta, A. and Amer, W. (2013). *“Clinical Chemistry, Immunology and Laboratory Quality Control”. A Comprehensive Review for Board Preparation, Certification and Clinical Practice.* Elsevier Publishing.

Dasgupta, A. and Wahed, A. (2014). "Gaussian Distribution and Reference Range". *Clinical Chemistry, Immunology and Laboratory Quality Control: Science Direct*, 47-66.

Duan, Y. and Li, D. (2020). "State Estimation". *Science Direct: Elservier Publishing*.

Ducker, M. J. (2015). *“The Fall of the F-Class Turbine”.* North America: Power Engineering International: Clarion Events.

El-Sehiemy, R. A., Hamida, M. A., Mesbahi, T. (2020). “Parameter Identification and State-of-Charge Estimation for Lithium-Polymer Battery Cells Using Enhanced Sunflower Optimization Algorithm”. . *International Journal of Hydrogen Energy.*, vol.45, Issue 15.

Franklin, W. (2020). *The Kalman Filter Explained Simply.* Retrieved from The Kalman Filter: https://thekalmanfilter.com/kalman-filter-explained-simply

Glenn, N. H. (2021). *“Burner Thermodynamics”.* Retrieved from National Aeronautics and Space Administration: www.nasa.gov/glenn

Glenn, N. H. (2023, January 21). *Properties of Air - Text Version.* Retrieved from National Aeronautics and Space Administration: www.ns.gov/glenn

Gupta, R. K., Pareek, U. and Kar, I. N. (2007). “Soft Computation of Turbine Inlet Temperature of Gas Turbine Power Plant Using Type-2 Fuzzy Logic System”. *IEEE International Fuzzy Systems Conference.* London, UK: IEEE.

Harman, R. T. (1981). *"Gas Turbine Engineering: Applications, Cycles and Characteristics".* . Macmillan.

Hellacioussatyr. (2024). *Heat Capacity Ratio: Revision History.* Retrieved from Specific Heat Capacity: https://en.m.wikipedia.org

Högnäs, T. (2005). *“Prediction of Fuel Gas Pressure Requirement for ALSTOM Heavy Duty Gas Turbines”.* Division of Heat and Power Engineering Lund Institute of Technology.: Lund University Publications.

Hou, D., Sun, Y., Wang, J., Zhang, L., Wang, S. (2023). “Dynamic State Estimation of Power Systems with Uncertainties Based on a Robust Adaptive Unscented Kalman Filter”. . *Journal of Modern Power Systems and Clean Energy.*, 1065-1074, vol. 11, No.4.

Hou, G., Gong, L., Dai, X., Wang, M., and Huang, C. . (2018). “A Novel Fuzzy Model Predictive Control of a Gas Turbine in the Combined Cycle Unit”. *Wiley Hindawi Online Library.*

I Love MATLAB. (Director). (2020). *"Kalman Filter in Matlab"* [Motion Picture]. Retrieved from www.youtube.com/@ilovematlab8485

Ibrahim, T. K. and Rahman, M. M. (2012). "Effect of Compression Ratio on Performance of Combined Cycle Gas Turbine". . *International Journal of Energy Engineering*, 2163 - 1905.

Impraimakis, M and Smyth, A. W. . (2022). "An Unscented Kalman Filter Method for Real Time Input-Parameter-State Estimation". *Elsevier Science Direct Journals & Books.*, vol. 162.

Impram, S., Nese, S. V. and Oral, B. (2020). "Challenges of Renewable Energy Penetration on Power System Flexibility: A Review". *Science Direct: Elservier Publishing.*

Instrument, Z. (2024). *"Understanding PID and APC Control Systems: A Detailed Overview".* Haitu Road Dalian Bonded Area, Pilot Ffree Trade Zone, Liaoning, China.

Jabbari, A., Zareinejad, M. and Ebrahim, A. (2015). "Modeling and Control of Gas Turbine Inlet Temperature using Adaptive Neuro-Fuzzy Inference System (ANFIS)". *IEEE Transactions on Energy Conversion.*

Jonatahan, . E., Olubiwe, M., Okozi, S. O., Agubor, C. K. (2018). "Exhaust Temperature Control of Heavy-Duty Gas Turbine Due to Incremental Load Demand". *International Journal of Engineering Research & Technology (ijert)*, Vol 07, Issue 07.

Kim, J. S., Powell, K. M., Edgar, T. F. (2013). "Nonlinear Model Predictive Control for a Heavy-Duty Gas Turbine Power Plant". *American Control Conference.* Washington DC.: IEEE.

Kurz, R. and Ohanian, S. (2003). "Modeling Turbomachinery in Pipeline Simulations". *Google Scholar*, PSIG 35th Annual General Meeting.

Larsson, E. (2014). "Model Based Diagnosis and Supervision of Industrial Gas Turbines". Department of Electrical Engineering, Linköping University, SE-581 83 , Linköping., Sweden.

Lo, W. L., Chung, H. S. H., Hsung, T. C., Fu, H. and Shen, T. W. (2023). "PV Panel Model Parameter Estimation by Using Neural Network." . *Sensors Journals, MDPI Publications, Switzerland.*, 1 - 19.

Manojkumar, R.; Jayaprakash, B.; and Nagaraju, P.V. . (2017). "An Overview of Power System State Estimation from Static State Estimation to Dynamic State Estimation". . *International Journal of Pure and Applied Mathematics.*, vol.114, No. 8.

Martinez, F. R., Martinez, A. A. R., Velázquez, M. T., Diez, P. Q., Eslava, G. T., and Francis, J. A. (2011). "Evaluation of the Gas Turbine Inlet Temperature with Relation to the Excess Air". *Energy and Power Engineering Journal.* , vol. 3. pp 517-524.

Mathworks. (2024). *Introduction to Estimation Filters.* Retrieved from Introduction to Estimation Filters - Mathworks: https://www.mathworks.com

Menon, E. S. (2011). "Pipeline Planning and Construction Manual". *Science Direct: Elservier*, 259 - 291.

Moura, S. (2018, February 14). "State Estimation". CE 295 - Energy Systems and Control, University of California, Berkeley.

Mouzinho, L. F., FonsecaNeto, J. V., Luciano, B. A. and Freire, R. C. S. (2006). "Indirect Measurement of the Temperature Via Kalman Filter". *Metrology for A Sustainable Development, XVIII IMEKO World Congress.*

Mukherjee, N. (2021, January 12). *"Adiabatic Process – A Short Review".* . Retrieved from Linkedin: https://www.linkedin.com/pulse/adiabatic-process-short-review-nikhilesh-mukherjee/

Nadeem, M., Nugroho, S. A. and Taha, A. F. . (2022). "Dynamic State Estimation of Nonlinear Differential Algebraic Equation Models of Power Networks." . *IEEE Transactions on Power Systems.*

Nigerian-Agip-Oil-Company. (2006). *"Fuel Gas System Description: ."*. Independent Power Plant, Okpai, Delta State, Nigeria: NAOC: Document Number: 1165-0-L-19-EKO-0-PES-101.

Nigerian-Agip-Oil-Company. (2024). "DCS Graphics". *Operator Stations: NAOC - OS3, NAOC - OS4*. Independent Power Plant, Okpai, Delta State, Nigeria.

Nigerian-Agip-Oil-Company. (2024). "Natural Gas Composition for Fuel Gas". *Emerson Process Management Config600 Remote Archive Uploader*. Independent Power Plant, Okpai, Delta State.

Nuclear-Power. (2025). *Thermal Efficiency - Brayton Cycle.* Retrieved from Thermal Efficiency Formula / Calculation: https://www.nuclear-power.com

Pathirathna, K. A. (2013). "Gas Turbine Thermodynamic and Performance Analysis Methods Using Available Catalog Data". . Faculty of Engineering and Sustainable Development., University of Ga¨vle., Sweden.

Pearson, J. (2014, November 24). "The Kalman Filter: An Unreasonably good State Estimator". *SIAM Seminar on Algorithms in Computational Science*. 1601 Elings Hall, University of California, Santa Barbara.

Ping, L., Xiangrui, K., Chen, F. and Zheng, Y. . (2019). "Novel Distributed State Estimation Method for AC-DC Hybrid Microgrid Based on the Lagrangian Relaxation Method". . *The Journal of Engineering: Institution of Engineering and Technology (IET*, Issue 18 / pp.4932-4936.

Pratt and Whitney. (1982). "The Aircraft Gas Turbine Engine and its Operation". *Oper. Instr. 200, United Technologies.*, 49.

Proctor II, C. L. (2003). "Brayton Cycle". *Encyclopaedia of Physical Science and Technology.*, (3rd Edition).

Qusai, Z., Al-Hamdan, and Munzer, S. Y. E. (2006). "Modeling and Simulation of Gas Turbine Engine for Power Generation". . *Journal of Engineering for Gas Turbines and Power*, Vol 128, Issue 2.

Rafi, M., Steck, J. E. and Watkins, J. . (2017). “Kalman-Filter-Based Adaptive Control: Flight Testing on General Aviation Aircraft”. . *Journal of Guidance, Control and Dynamics, American Institute of Aeronautics and Astronautics.*, Vol. 40, No 4.

Rao, R. J. (2017). “Advanced Process Control (APC). . *Instrumentation Tools.* Retrieved from Infohe.com.

RealPars. (2019). *“What is a Gas Turbine.?”*. Retrieved from Youtube: https://www.youtube.com/watch.

Rehan, A., Ahmad, R. and Rehan, S. (2016). “Non-linear Estimation and Control of Gas Turbine Inlet Temperature Using Sliding-Model Technique”. *Journal of Control, Automation and Electrical System.*

RH. (2018, June 19). *Kalman filters vs. state observers*. Retrieved from Engineering Stack Exchange: engineering.stackexchange.com

Roberts, M. J. (2010). “State Space Analysis”.. . *Esa Journals: Wiley.*

Salim, B., Orfi, J. and Alaqel, S. S. . (2020). "Effect of Turbine and Compressor Inlet Temperatrures and Air Bleeding on the Comparative Performance of Simple and Combined Gas Turbine Unit". *European Journal of Engineering Research and Science.*, Vol.5, No. 12.

Sharifi, A. and Salarieh, H. . (2023). “An Adaptive Synergetic Controller Applied to Heavy-Duty Gas Turbine Unit.” . *Science Direct Journals & Books. Elsevier Publishing on Applied Energy.*, vol. 333.

Sharma, S., Dwived, V. and Das, S. (2017). “Estimation of Gas Turbine Inlet Temperature Using Extended Kalman Filter”. *International Journal of Electrical Power and Energy Systems.*

SPE. (2023). *“Compressors”.* . Society of Petroleum Engineers [SPE] International. PetroWiki.

Subramaniam, G. (2018). *"Why is Heat Capacity at Constant Pressure always greater than Heat Capacity at Constant Volume?'.* Retrieved from https://physics.bu.edu/

Sudev, P.; Anita, J. P. and Sudheesh, P. (2017). “Nonlinear State Estimation of Wind Turbine”. *IEEE International Conference on Advances in Computing, Communications and Informatics (ICACCT).* Udupi, India: IEEE.

Sundén, Bengt and Fu, Juan. (2017). "Heat Transfer in Aerospace Applications". *Elservier: ScienceDirect Journals & Books*, pp. 197-230.

Testbook. (2023, November 16). *Gas Turbine: Know Definition, Components, Working, Types.* Retrieved from Testbook: https://www.testbook.com

Tiwari, S. R. (2015, February 19). “Kalman Filter 101: State Estimation”. . *Matlab Helper*. Tellmate Helper Private Limited.

Tree, D. R., Badger, D., Zeltner, D. and Rezasoltani, M. (2022). "Turbine Inlet Temperature Measurements in an 8200 KW Gas Turbine Using Water Vapor Emission". *Journal of Engineering for Gas Turbines and Power: ASME.*, 1528-8919.

Trivedi, T. (2018, January 17). “Controllability and Observability”. , . Electrical Engineering Department, Marwadi Education Foundation Group of Institutions, Rajkot., Gujarat, India.

Ulusoy, M. (2018). “Why use Model Predictive Control/Understanding Model Predictive Control Part 1”. *MATLAB Tech Talks, http://bit.ly/2xfEe2M*. MathWorks Inc.

Venkateswarlu, Ch. and Karri, R. R. (2022). "Optimal State Estimation for Process Monitoring, Fault Diagnosis and Control". *Science Direct: Elservier*.

Vinodh, K. E., Jerome, J. and Ayyappan, S. . (2013). “Comparison of Four State Observer Design Algorithms for MIMO System". *Archives of Control Sciences.*, vol 23 (2) pp131-144.

Wärtsilä. (2021). *Gas turbine technology.* Retrieved from Combustion engine vs. Aeroderivative gas turbine - Introduction - Wärtsilä: https://www.wartsila.com/energy

Weber, B. (2019). “Applied Thermodynamics”. . Mechanical Engineering Department, University of Connecticut, New York, U.S.A.

Whittle, F., Ohian, H. J. P., and Bell, L. D. (2025). "Theoretical Study on Jet Engines". *International Journal of Advance Research and Innovative Ideas in Education.*

Xiao, R., Wang, G., Hao, X., Huang, R. and Xiong, Y. (2020). “Dynamic State Estimation of Medium-Voltage DC Integrated Power System with Pulse Load”. *Journal of Modern Power Systems and Clean Energy*, vol. 8, No. 4.

Yaghoubi, M., Eslami, M., Noroozi, M., Mohammadi, H., Kamari, O. and Palani, S. (2022). “Modified Salp Swarm Optimization for Parameter Estimation of Solar PV Models”. *IEEE Access*, vol. 10, pp. 110181-110194.

Young, H. D. (2012). “University Physics (13th Edi.) Solutions". *StudySoup*. Pearson Education Line: Addison - Wesley. ISBN: 978-0-321-69686-1.

Yousef, S. H. N. and Abubakar, A. M. (2015). "Indirect Evaporative Combined Inlet Air Cooling with Gas Turbines for Green Power Technology". *International Journal of Refrigeration*, vol. 59, pp. 235-250.

Zeng, L., Dong, S. and Long, W. . (2019). “The Rotating Components Performance Diagnosis of Gas Turbine Based on the Hybrid Filter”. . *Special Issue Optimization for Control, Observation and Safety: MPPI Journals.* , EISSN 2227-9717.

Zohuri, B. (2018). “Chapter 6 Thermodynamics of Cycles”. *Galaxy Advanced Engineering: https://www.researchgate.net/publication* .

APPENDIX A

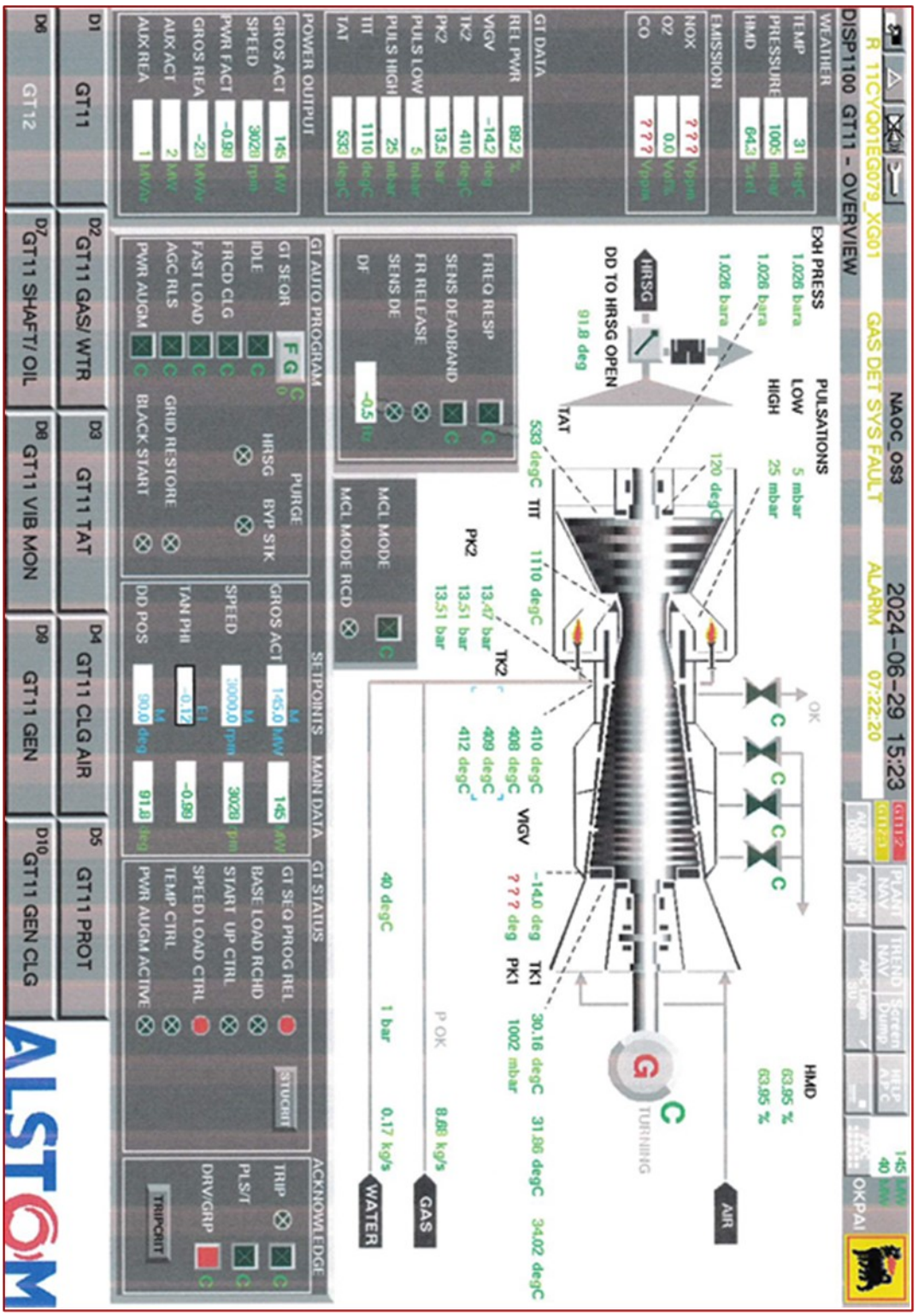

Plate 3.1: DCS Graphics from GT11 Life Plant (NAOC, 2024)

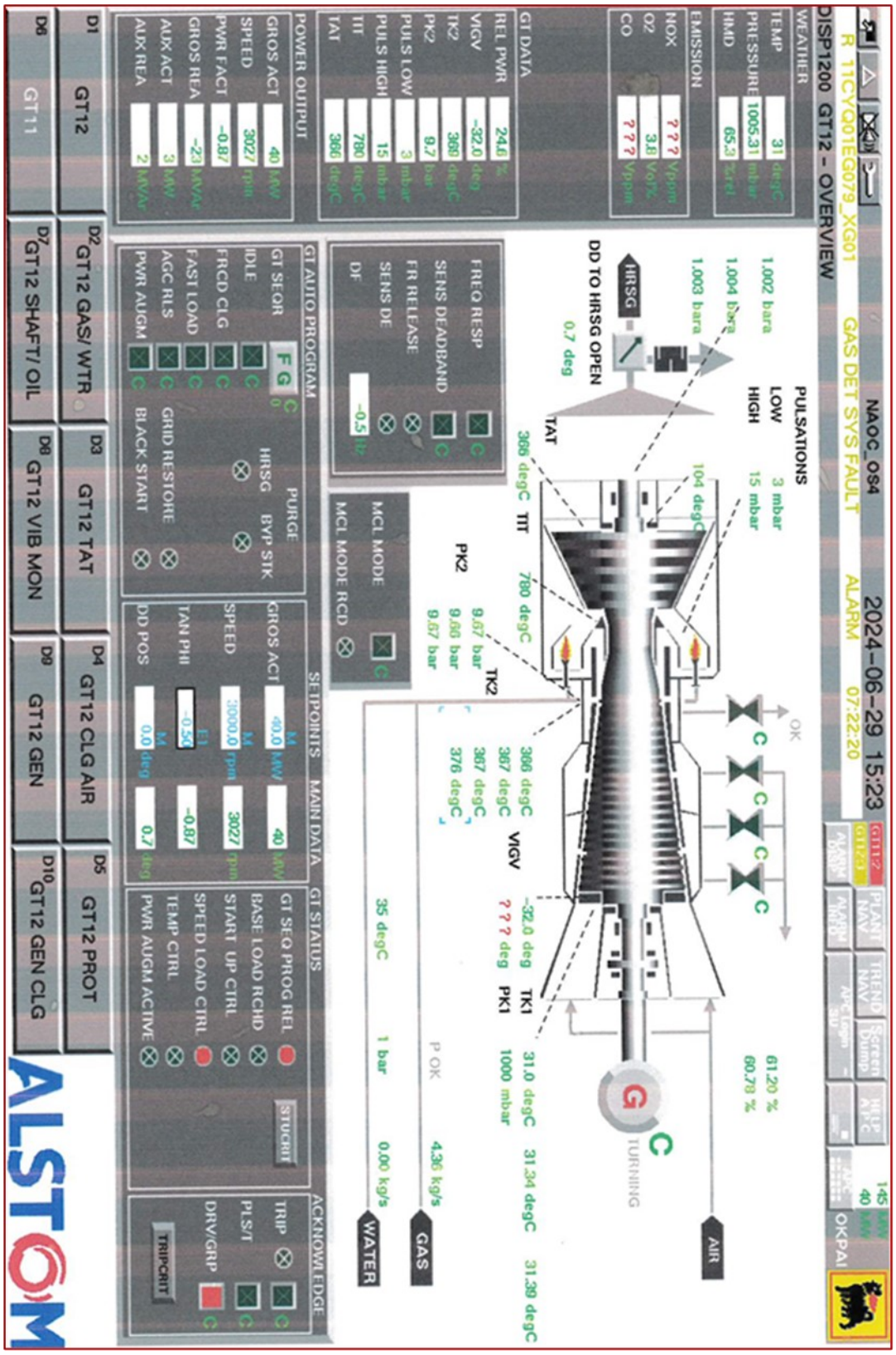

Plate 3.2: DCS Graphics from GT12 Life Plant (NAOC, 2024)

APPENDIX B

MATLAB Program Code for GT11 Model.

```
% % This function implements a Kalman filter model
% % The Kalman filter estimates the inlet temperature (T3) of a gas turbine
% % Author: Francis Usen (FUTO, 2024)
% % Defining Parameters for the state space
open system ('TITSim');
Ts = 0.1;
cp = 1005;
mf = 8680;
ma = 277760;
f = (ma/mf);
Hv = 39600520;
T2 = 410;
nt = 0.83;
T3 = (cp*T2 + nt*Hv*f)/(cp*(1+f));
z = (ma*cp)/(mf*Hv);
u = [0 1]';
% % Measurement Noise Variance
MNstd = 0.05;
MNV = MNstd*MNstd;
% % Measurement Noise Covariance Matrix
R = eye(1)*MNV;
% % Process Noise Variance
PNstd = 0.02;
PNV = PNstd*PNstd;
% % Process Noise Covariance Matrix
Q = eye(2)*PNV;
% % Defining the state space model
A = [0, 0; 0, -((1+f)/cp*(1+f)*z)];
B = [0, 0; 1, 0];
C = eye(2);
D = 0;
% % Create SS System
ss_model = ss(A, B, C, D);
step(ss_model);
% % Do initialization
xhat = 0;
yhat = ss(A,B,C,D);
P = 0;
% % Propagate the state estimate and covariance matrix;
P = A*P*A' + Q;
% % Calculate the Kalman gain
K = P*C'/(C*P*C' + R);
% % update the state and error covariance estimate
P = (eye(size(K,1)) - K*C)*P;
% % Post the results
sim('TITSim');
```

MATLAB Program Code for GT12 Model.

```
% % This function implements a Kalman filter model
% % The Kalman filter estimates the inlet temperature (T3) of a gas turbine
% % Author: Francis Usen (FUTO, 2024)
% % Defining Parameters for the state space
open system ('TITSim');
Ts = 0.1;
cp = 1005;
mf = 4360;
ma = 156960;
f = (ma/mf);
Hv = 39600520;
T2 = 369;
nt = 0.79;
T3 = (cp*T2 + nt*Hv*f)/(cp*(1+f));
z = (ma*cp)/(mf*Hv);
u = [0 1]';
% % Measurement Noise Variance
MNstd = 0.05;
MNV = MNstd*MNstd;
% % Measurement Noise Covariance Matrix
R = eye(1)*MNV;
% % Process Noise Variance
PNstd = 0.06;
PNV = PNstd*PNstd;
% % Process Noise Covariance Matrix
Q = eye(2)*PNV;
% % Defining the state space model
A = [0, 0; 0, -((1+f)/cp*(1+f)*z)];
B = [0, 0; 1, 0];
C = eye(2);
D = 0;
% % Create SS System
ss_model = ss(A, B, C, D);
step(ss_model);
% % Do initialization
xhat = 0;
yhat = ss(A,B,C,D);
P = 0;
% % Propagate the state estimate and covariance matrix;
P = A*P*A' + Q;
% % Calculate the Kalman gain
K = P*C'/(C*P*C' + R);
% % update the state and error covariance estimate
P = (eye(size(K,1)) - K*C)*P;
% % Post the results
sim('TITSim');
```